

**$v_1$ -PERIODIC MOTIVIC HOMOTOPY OVER PRIME FIELDS**

HANA JIA KONG AND J.D. QUIGLEY

ABSTRACT. We compute the motivic stable homotopy groups of a variant of the connective image-of- $J$  spectrum over prime fields of characteristic not two. Together with the analogous computation over algebraically closed fields, this yields information about  $v_1$ -periodic motivic stable homotopy groups over arbitrary base fields of characteristic not two.

## CONTENTS

1. Introduction	1
2. Background	5
3. Coefficient rings of $H\mathbb{Z}/2^n$	10
4. Coefficient rings of $kq$	12
5. Coefficient rings of $L$ over prime fields	15
Appendix A. Figures	20
References	29

## 1. INTRODUCTION

Motivic stable homotopy theory, or the stable homotopy theory of algebraic varieties, was developed by Morel and Voevodsky in [MV99] to apply powerful techniques from stable homotopy theory to problems in algebraic geometry and number theory. Since motivic stable homotopy groups are the universal stable  $\mathbb{A}^1$ -invariant, a great deal of effort has gone into understanding the *motivic stable stems*, i.e., the motivic stable homotopy groups of the unit in the motivic stable homotopy category. This paper studies certain patterns in an approximation to the motivic stable stems over prime fields of characteristic not two. Using analogous results over algebraically closed fields, this establishes the existence of similar patterns over arbitrary base fields of characteristic not two.

To situate our results, we briefly survey the existing analyses of the motivic stable stems. Over arbitrary base fields, the low-dimensional Milnor–Witt stems<sup>1</sup> are connected to Milnor–Witt K-theory [Mor12] and Milnor K-theory, Hermitian K-theory, and motivic cohomology [RSØ19, RSØ21]. Over certain base fields, various completions of the motivic stable stems have been computed in larger ranges [BCQ21, BI22, DI10, DI17b, Isa19, IWX20, OØ14, Wil16, WØ17].

The most well-studied pattern in the motivic stable stems is  $\eta$ -periodicity, where  $\eta$  is the first motivic Hopf map. The  $\eta$ -periodic motivic stable stems have been computed over various base fields [AM17, CQ21, GI15, GI16, OR20, Wil18]. Over general base fields and

<sup>1</sup>The  $n$ -th Milnor–Witt stem is the sum over  $i \in \mathbb{Z}$  of  $\pi_{n+i,i}^F(\mathbb{S})$ , where  $\mathbb{S}$  is the unit. See Section 1.4 for our indexing conventions on motivic stable homotopy groups.

Dedekind domains, the  $\eta$ -periodic sphere spectrum sits in a fiber sequence with connective Witt theory [BH20, Bac22].

The pattern we study in this paper,  $v_1$ -periodicity, is much less well-understood. The  $v_1$ -periodic motivic stable stems have been computed over the algebraically closed fields of characteristic zero [CQ21], and a small number of  $v_1$ -periodic families have been produced over general base fields [Qui21a, Qui21b]. In [BIK22], the coefficients of a motivic spectrum  $L$  which captures the  $v_1$ -periodic phenomena in the motivic stable stems (cf. Remark 1.1) are computed over the complex numbers and the real numbers.

Our main result (Theorem A) is a computation of the coefficients of  $L$  over all prime fields of characteristic not two and all algebraically closed fields. Since any field sits between a prime field and an algebraically closed field in a sequence of field extensions, our computations identify the  $v_1$ -periodic phenomena which is present over every base field of characteristic not two.

**1.1. Summary of results.** From now on, we work in the 2-complete setting and only work over base fields  $F$  of characteristic not two. In [BH20], Bachmann and Hopkins defined Adams operations on the very effective cover of Hermitian K-theory [ARØ20]

$$\psi^3 : kq \rightarrow kq.$$

Following [BIK22], we define a motivic spectrum  $L$  by

$$L := \text{fib}(\psi^3 - 1 : kq \rightarrow kq).$$

**Remark 1.1.** In classical stable homotopy theory, the  $v_1$ -periodic stable stems are captured by the connective cover of the  $K(1)$ -local sphere,  $\tau_{\geq 0}L_{K(1)}\mathbb{S}$ , where  $L_{K(1)}$  denotes Bousfield localization with respect to the first Morava K-theory. It is believed that  $L$  is a motivic analogue of a slight variant of  $\tau_{\geq 0}L_{K(1)}\mathbb{S}$ , and thus the coefficients  $\pi_{**}^F(L)$  can be thought of as the “ $v_1$ -periodic  $F$ -motivic stable stems.” In fact, over  $F = \mathbb{C}$ , the Betti realization of  $L$  is equivalent to  $\tau_{\geq 0}L_{K(1)}\mathbb{S}$  above degree 2.<sup>2</sup> Moreover, over algebraically closed fields  $F = \bar{F}$  of characteristic zero, the groups  $\pi_{**}^F(L)$  (computed in [BIK22]) coincide with the  $v_1$ -periodic  $F$ -motivic stable stems (computed in [CQ21]) above topological degree 2.

Our main result is the following:

**Theorem A.** The groups  $\pi_{**}^F(L)$  are described in Section 5 for the following base fields  $F$ :

- (1) For  $F = \bar{F}$  algebraically closed in Section 5.1.
- (2) For  $F = \mathbb{F}_q$  a finite field of characteristic not two in Section 5.2.
- (3) For  $F = \mathbb{Q}_q$  in Section 5.3 ( $q$  odd) and Section 5.4 ( $q = 2$ ).
- (4) For  $F = \mathbb{R}$  in Section 5.5.
- (5) For  $F = \mathbb{Q}$  in Section 5.6.

**Remark 1.2.** The groups  $\pi_{**}^F(L)$  were already computed for  $F = \mathbb{C}$  and  $F = \mathbb{R}$  by Belmont, Isaksen, and the first author in [BIK22], so our new contribution is the computation over prime fields and the  $q$ -adic rationals.

One simple consequence of our computations is that a famous pattern of 2-torsion in the classical stable stems sits in  $\pi_{**}^F(L)$  for all fields  $F$ .

<sup>2</sup>The motivic image-of- $J$  spectrum  $j$  (see Remark 2.1) is equivalent in all degrees, but for some technical reasons explained in [BIK22, Introduction], we will work with  $L$  instead of  $j$ .

**Corollary 1.3.** *Let  $F$  be any field of characteristic not two. Then  $\pi_{4k-1,2k}^F(L)$  contains a summand of order at least the 2-component of  $\text{denom}\left(\frac{B_{2k}}{4k}\right)$ , where  $B_{2k}$  is the  $2k$ -th Bernoulli number.*

*Proof.* Any field  $F$  sits in a sequence of field extensions

$$k \rightarrow F \rightarrow \bar{F}$$

between a prime field  $k$  and its algebraic closure  $\bar{F}$ . Inspecting the results of Section 5, we see that the corollary holds for  $k$  and  $\bar{F}$ , and moreover, the relevant summands in  $k$  base change to the corresponding summands in  $\bar{F}$ . It follows by naturality that they must be nonzero in  $F$ .  $\square$

**Remark 1.4.** More generally, the groups  $\pi_*(\tau_{\geq 0}L_{K(1)}\mathbb{S})$  appear as subgroups of  $\pi_{**}^F(L)$  in bidegrees approximately of the form  $(2n, n)$  for all primes fields and algebraically closed fields. Therefore the classical  $v_1$ -periodic stable stems sit interestingly inside  $\pi_{**}^F(L)$  for all fields of characteristic not two. In particular, we recover the  $v_1$ -periodic elements constructed in [Qui21a, Qui21b].

Corollary 1.3 and Remark 1.4 highlight some features of  $v_1$ -periodic motivic stable homotopy theory which are independent of the base field. We include the following remark to illustrate an aspect of the computation which does depend on the base field.

**Remark 1.5.** As we will explain below, we compute  $\pi_{**}^F(L)$  using the effective slice spectral sequence. When  $F = \mathbb{C}$ , there is an important family of  $d_1$ -differentials

$$d_1(\iota v_1^2 \tau^n) = \iota \tau^{n+1} h_1^3$$

which occur for all  $n \geq 0$ . However, when  $F = \mathbb{F}_q$ , the similar differential  $d_1(\iota x_q v_1^2 \tau^n)$  occurs if and only if

$$\begin{cases} \nu(q-1) + \nu(n+1) > 3 & \text{if } q \equiv 1 \pmod{4}, \\ \text{unconditionally} & \text{if } q \equiv 3 \pmod{4} \text{ and } n \equiv 0 \pmod{2}, \\ \nu(q^2-1) + \nu(n+1) > 4 & \text{if } q \equiv 3 \pmod{4} \text{ and } n \equiv 1 \pmod{2}, \end{cases}$$

where  $\nu(-)$  denotes dyadic valuation. Further discussion appears in Section 5.2.

We compute  $\pi_{**}^F(L)$  over prime fields using the effective slice spectral sequence (ESSS), a powerful tool which has been used to great effect in recent years (e.g., [KRØ20, RØ16, RSØ19, RSØ21]). The  $E_1$ -term of the ESSS for  $L$  is comprised of shifted copies of  $\pi_{**}^F(H\mathbb{Z}/2^n)$  for varying  $n$ . The coefficient rings of  $H\mathbb{Z}/2$  and  $H\mathbb{Z}$  have been recorded over prime fields [Hil11, Orm11, OØ13, Kyl15] (see Section 2 for a summary), but as far as we are aware, the coefficient rings of  $H\mathbb{Z}/2^n$  have not appeared in previous literature.

**Theorem B.** The groups  $\pi_{**}^F(H\mathbb{Z}/2^n)$  are described for all  $n \geq 1$  and all  $F \in \{\bar{F}, \mathbb{F}_q, \mathbb{Q}_q, \mathbb{R}, \mathbb{Q}\}$  in Section 3.

Even with these groups in hand, describing the  $E_1$ -term of the ESSS for  $L$  in a manner suitable for computations is a difficult problem. One novel aspect of our work is the concise graphical calculus developed in Section 4 and Section 5. Previous computations over  $\mathbb{F}_q$  (e.g., [Kyl15, WØ17]) or  $\mathbb{Q}_q$  (e.g., [OØ13]) often use different charts to display information for different congruence classes of  $q$ , while computations over  $\mathbb{R}$  (e.g., [BI22, DI17a, BIK22]) usually use different charts for different Milnor–Witt stems. In our work, however, we are

able to display complicated data, like the  $E_1$ -page of the ESSS for  $L$  over  $\mathbb{F}_q$ ,  $q$  odd, in a single chart (Figure 13).<sup>3</sup>

Once we have described the  $E_1$ -term of the ESSS for  $L$ , we are tasked with computing differentials. In all of the cases we consider, the differentials are forced by comparison with the ESSS for  $L$  over algebraically closed fields, the ESSS for  $kq$  over the given prime field, or in the case  $F = \mathbb{Q}$ , comparison with the ESSS for  $L$  over  $\mathbb{R}$  and  $\mathbb{Q}_q$ .

**Theorem C.** The effective slice spectral sequence for  $kq$  is explicitly described in Section 4 for the following base fields:

- (1) For  $F = \bar{F}$  algebraically closed in Section 4.1.
- (2) For  $F = \mathbb{F}_q$  a finite field in Section 4.2.
- (3) For  $F = \mathbb{Q}_q$  in Section 4.3 ( $q$  odd) and Section 4.4 ( $q = 2$ ).
- (4) For  $F = \mathbb{R}$  in Section 4.5.
- (5) For  $F = \mathbb{Q}$  in Section 4.6.

**Remark 1.6.** The effective slice spectral sequences for  $kq$  over  $F = \bar{F}$  and  $F = \mathbb{R}$  were already described in [BIK22]. In fact, [RØ16], Røndigs and Østvær expressed the differentials in the ESSS for  $kq$  in terms of Steenrod operations over any field of characteristic not two. Theorem C provides the more explicit analysis in terms of generators and relations needed to analyze the ESSS for  $L$ .

While describing *how* the differentials in the ESSS for  $L$  are produced is easy, actually determining *which* differentials occur and describing the pattern intelligibly is difficult. As we alluded to in Remark 1.5, the characteristic of the base field (or its residue field) determines whether or not certain  $d_1$ -differentials occur. Our approach is to find arithmetic conditions under which differentials occur, and then describe the groups in the next page of the ESSS in terms of these conditions. We refer the reader to Section 5.2 for examples and further discussion.

**Remark 1.7.** One consequence of our analysis is that the Hasse map

$$\pi_{**}^{\mathbb{Q}}(E) \rightarrow \prod_{\nu} \pi_{**}^{\mathbb{Q}_{\nu}}(E),$$

where  $\nu$  ranges over all places, is injective for  $E = kq$  and  $E = L$ . In the terminology of Ormsby–Østvær [OØ13],  $kq$  and  $L$  satisfy the motivic Hasse principle. In [BCQ21], Balderrama, Culver, and the second author showed that the  $E_2$ -term of the motivic Adams spectral sequence converging to the motivic stable stems satisfies the motivic Hasse principle. Since  $kq$  and  $L$  serve as first approximations to the motivic sphere spectrum, it is interesting to wonder if the motivic sphere spectrum itself might satisfy the motivic Hasse principle.

**Remark 1.8.** In [OØ13, Rmk. 5.14], Ormsby–Østvær explain how their computation of  $\pi_{**}^{\mathbb{Q}}BPGL\langle 1 \rangle$  and [OØ13, Lem. 2.9] can be used to recover the Rognes–Weibel computation of the 2-complete algebraic K-theory of  $\mathbb{Q}$  from [RW00]. Similarly, our computations can be used to recover the 2-complete Hermitian K-theory of  $\bar{F}$ ,  $\mathbb{F}_q$ ,  $\mathbb{Q}_q$ ,  $\mathbb{R}$ , and  $\mathbb{Q}$  using [Kyl15, Lem. 1.5.12] which relates  $\pi_{**}kq$  to  $\pi_{**}KQ$ . For example, using Theorem C, we can recover some of the Hermitian K-theory computations of Friedlander [Fri76] and Berrick–Karoubi [BK05].

<sup>3</sup>Roughly speaking, the tradeoff is that instead of using multiple charts containing a small variety of symbols, we use a single chart containing a large variety of symbols.

**1.2. Forthcoming work.** In a forthcoming companion paper [KQ22], we analyze the coefficients of  $L$  over rings of  $S$ -integers in number fields, where  $S$  contains the archimedean and dyadic places. In contrast with the explicit computations carried out in this paper, which mirror the generator-and-relation approach employed in [BIK22], our approach in [KQ22] takes a more abstract approach, identifying  $\pi_{***}^{O_{F,S}} L$  in terms of arithmetic invariants like motivic cohomology and Steenrod operations. This approach builds on the ideas introduced by Röndigs–Spitzweck–Østvær in their computations of the first and second motivic stable stems [RSØ19, RSØ21] and Kylling–Röndigs–Østvær in their analysis of the Hermitian K-theory of Dedekind domains [KRØ20]. Based on the computations in *loc. cit.*, we expect that the special values of Dedekind zeta functions can naturally be related to the coefficients of  $L$  using this approach.

**1.3. Outline.** In Section 2, we recall the spectrum  $L$  and its essential properties. We also recall the coefficients of  $H\mathbb{Z}/2$  and  $H\mathbb{Z}$  over our fields of interest.

In Section 3, we compute the coefficient rings of  $H\mathbb{Z}/2^n$  for all  $n \geq 1$  over the relevant fields. Our approach using the Adams spectral sequence may be of independent interest.

In Section 4, we recall the ESSS for  $kq$  over algebraically closed fields and the reals from [BIK22], and explicitly describe the ESSS for  $kq$  over prime fields and the  $q$ -adic rationals. The results in this section are used in Section 5 to produce some differentials in the next section.

In Section 5, we recall the ESSS for  $L$  over algebraically closed fields and the reals from [BIK22], and analyze the ESSS for  $L$  over prime fields and the  $q$ -adic rationals.

**1.4. Conventions.**

- (1) We implicitly work in the 2-complete setting.
- (2) We work over fields of characteristic not two. In particular,  $\mathbb{F}_q$  always refers to a finite field of odd characteristic.
- (3) Motivic stable homotopy groups are bigraded in the form  $(s, w)$ , where  $s$  denotes the stem and  $w$  denotes the motivic weight.
- (4) We use the abbreviation ‘ESSS’ for the effective slice spectral sequence.
- (5) We write  $s_*(X)$  for the slices of a motivic spectrum  $X$ .
- (6) The horizontal axis in ESSS charts is always the stem  $s$  and the vertical axis is always the “Adams–Novikov filtration”  $f$ , which is twice the effective slice filtration minus the stem.
- (7)  $E_r^F(X)$  denotes the  $E_r$ -page of the ESSS for an  $F$ -motivic spectrum  $X$ . If the field is understood, we will sometimes suppress it from the notation.
- (8) We take the elements  $h$  and  $\rho$  to be as defined in the conventions of [BIK22].

**1.5. Acknowledgments.** The authors thank Oliver Röndigs for discussions related to [KRØ20] and a reminder about the convergence of the ESSS. The first author was supported by National Science Foundation grant DMS-1926686. The second author is grateful to the Max Planck Institute for Mathematics in Bonn for its hospitality and financial support.

2. BACKGROUND

In this section, we provide the background necessary for our computations. The motivic spectrum  $L$  and its essential properties are recalled in Section 2.1, and the coefficients of

the Eilenberg–MacLane spectra  $H\mathbb{Z}/2$  and  $H\mathbb{Z}$  over our fields of interest are recalled in Section 2.2.

**2.1. The motivic spectrum  $L$  and its slices.** In [BH20], Bachmann and Hopkins constructed a unital ring map

$$\psi^3 : kq \left[ \frac{1}{3} \right] \rightarrow kq \left[ \frac{1}{3} \right]$$

whose Betti realization is the classical Adams operation  $\psi^3$ . We define

$$L := \text{fib} \left( \psi^3 - 1 : kq \left[ \frac{1}{3} \right] \rightarrow kq \left[ \frac{1}{3} \right] \right).$$

We will use the effective slice spectral sequence (ESSS) [Lev08, RSØ19]

$$E_1^{s,f,w}(X) = \pi_{s,w}(s_{\frac{s+f}{2}}(X)) \Rightarrow \pi_{s,w}(X)$$

to study  $\pi_{**}^F L$  for various base fields  $F$ . The differentials in the ESSS have the form

$$d_r : E_r^{s,f,w} \rightarrow E_r^{s-1, f+2r-1, w},$$

cf. [BIK22, Thm. 2.7].

The  $E_1$ -page of the ESSS for  $L$  can be computed using the fiber sequence of slices

$$s_* L \rightarrow s_* kq \xrightarrow{\psi^3 - 1} s_* kq,$$

which implies

$$\pi_{**} s_* L \cong K \oplus \Sigma^{-1} C$$

where

$$K := \ker(\pi_{**}(\psi^3 - 1)) \quad \text{and} \quad C := \text{coker}(\pi_{**}(\psi^3 - 1)).$$

As in [BIK22], we will write  $\iota x$  for the image of  $x \in \Sigma^{-1} C$  under the inclusion into  $\pi_{**} s_* L$ .

We use the grading convention  $(s, f_{AN}, w)$  as in [BIK22]. Here  $s$  is the stem,  $w$  is the weight, and  $f_{AN}$  is the “Adams–Novikov filtration”, which equals twice the stem minus the slice filtration  $2f - s$ .

By [ARØ20, Thm. 17], the slices of  $kq$  can be expressed by the formula

$$(1) \quad s_* kq = H\mathbb{Z}[h_1, v_1^2]/(2h_1),$$

where  $|v_1^2| = (4, 0, 2)$  and  $|h_1| = (1, 1, 1)$ . We explain the meaning of this formula. In  $H\mathbb{Z}[h_1, v_1^2]/(2h_1)$ , a monomial of tri-degree  $(s, f_{AN}, w)$  contributes a summand of the motivic Eilenberg–MacLane spectrum  $\Sigma^{s,w} HA$  to the  $w$ th slice  $s_w kq$ .

**Remark 2.1.** In [BH20], Bachmann and Hopkins showed that the map  $\psi^3 - 1$  factors

$$(2) \quad kq \xrightarrow{\psi^3 - 1} \Sigma^{4,2} ksp$$

where the target is the very effective cover of  $\Sigma^{4,2} kq$ . After localizing at 2, the fiber of (2) defines a motivic spectrum  $j$  that is analogous to the classical image-of- $J$  spectrum.

It can be shown that the slices of  $j$  can be expressed by

$$s_* j = H\mathbb{Z} \otimes \{\alpha\text{-family classes}\}$$

where “ $\alpha$ -family classes” refers to the classical Adams–Novikov classes (at the prime 2) in filtration 1 and their  $\alpha_1$ -power multiples.

The slices of  $L$  and  $j$  differs by a tower of suspensions of  $H\mathbb{F}_2$ , and in slice filtrations  $-1$  and  $2$ . More precisely, the very effective cover functor gives  $\Sigma^{4,2}ksp \rightarrow kq$ , which induces a map  $j \rightarrow L$ . The difference between  $s_*L$  and  $s_*j$  is given by

$$s_* \operatorname{cofib}(j \rightarrow L) = H\mathbb{Z} \otimes \left( \mathbb{Z}[h_1]/(2h_1)\{\iota\} \oplus \mathbb{F}_2\{\bar{\alpha}_2\} \right)$$

where  $|\iota| = (-1, 1, 0)$  and  $|\bar{\alpha}_2| = (3, 1, 2)$ .

One can compute the coefficients of  $j$  over prime fields using the techniques in this manuscript, but the computation is slightly messier in low degrees.

**Theorem 2.2.** *Over the base fields  $F = \bar{F}, \mathbb{F}_q, \mathbb{Q}_q, \mathbb{R}, \mathbb{Q}$ , the slice spectral sequence for  $L$  and the slice spectral sequence for  $kq$  converge strongly to  $\pi_{**}^F(L_2^\wedge)$  and  $\pi_{**}^F(kq_2^\wedge)$ .*

*Proof.* The case for  $\mathbb{R}$  is proved in [BIK22]. By [BIK22], the limit of the 2-completed slice tower of  $L$  is  $(2, \eta)$ -completed  $L$ . Over the specified base fields, the  $(2, \eta)$ -completions of  $L$  and  $kq$  coincide with the 2-completions of  $L$  and  $kq$  by [HKO11] (in characteristic zero) and [WØ17, Prop. 5.10] (in positive characteristic). The result then follows from [Boa99, Thm. 7.1] and the calculations in §4 for  $kq$  and §5 for  $L$ .  $\square$

**2.2. Coefficient rings of  $H\mathbb{Z}/2$  and  $H\mathbb{Z}$ .** For future reference, we record the coefficient rings of  $H\mathbb{Z}/2$  and  $H\mathbb{Z}$  over various base fields in this section. We refer the reader to [IØ20, Sec. 2.1] for a summary of how  $\pi_{**}^F(H\mathbb{Z}/2)$  can be computed using Milnor K-theory [Mil70] and the Bloch–Kato Conjecture [Voe03, Voe11]. All of the computations of  $\pi_{**}^F(H\mathbb{Z}/2)$  appear in [IØ20], except the case  $F = \mathbb{Q}$  which we pull from [OØ13]. Once  $\pi_{**}^F(H\mathbb{Z}/2)$  is known, the groups  $\pi_{**}^F(H\mathbb{Z})$  can be computed using the  $\rho$ -Bockstein spectral sequence [Hil11] and motivic Adams spectral sequence [DI10], or by consulting previous motivic cohomology computations.

**2.2.1. Algebraically closed fields.** These results follow, for instance, from [DI10]. Let  $F = \bar{F}$  be an algebraically closed field. Then we have

$$\pi_{**}^F(H\mathbb{Z}/2) \cong \mathbb{Z}/2[\tau], \quad \pi_{**}^F(H\mathbb{Z}) \cong \mathbb{Z}_2[\tau],$$

where  $|\tau| = (0, -1)$ .

**2.2.2. Finite fields.** These results appear, for instance, in [Kyl15]. We have

$$\pi_{**}^{\mathbb{F}_q}(H\mathbb{Z}/2) \cong \begin{cases} \mathbb{Z}/2[\tau, u]/(u^2) & \text{if } q \equiv 1 \pmod{4}, \\ \mathbb{Z}/2[\tau, \rho]/(\rho^2) & \text{if } q \equiv 3 \pmod{4}, \end{cases}$$

and

$$\pi_{**}^{\mathbb{F}_q}(H\mathbb{Z}) \cong \begin{cases} \mathbb{Z}\{1\} \oplus \bigoplus_{i \geq 0} \mathbb{Z}/2^{\nu(q-1) + \nu(i+1)}\{u\tau^i\} & \text{if } q \equiv 1 \pmod{4}, \\ \mathbb{Z}\{1\} \oplus \bigoplus_{i \geq 0, \text{ even}} \mathbb{Z}/2\{\rho\tau^i\} \\ \bigoplus \bigoplus_{i \geq 0, \text{ odd}} \mathbb{Z}/2^{\nu(q^2-1) + \nu(i+1)-1}\{\rho\tau^i\} & \text{if } q \equiv 3 \pmod{4}, \end{cases}$$

where  $|\tau| = (0, -1)$  and  $|u| = |\rho| = (-1, -1)$ .

In order to make our analysis of finite fields independent of the congruence class of  $q$ , we make the following definition.

**Definition 2.3.** For all  $i \geq 0$  and odd prime powers  $q$ , we define

$$s_q(i) := \begin{cases} \nu(q-1) + \nu(i+1), & \text{if } q \equiv 1 \pmod{4}, \\ 1 & \text{if } q \equiv 3 \pmod{4} \text{ and } i \equiv 0 \pmod{2}, \\ \nu(q^2-1) + \nu(i+1) - 1 & \text{if } q \equiv 3 \pmod{4} \text{ and } i \equiv 1 \pmod{2}. \end{cases}$$

With this notation, we have for all odd prime powers  $q$  that

$$\pi_{**}^{\mathbb{F}_q}(HZ) \cong \mathbb{Z}\{1\} \oplus \bigoplus_{i \geq 0} \mathbb{Z}/2^{s_q(i)}\{x_q \tau^i\},$$

where  $x_q = u$  if  $q \equiv 1 \pmod{4}$  and  $x_q = \rho$  if  $q \equiv 3 \pmod{4}$ .

2.2.3.  $\mathbb{Q}_q$  with  $q$  odd. These results appear in [Orm11]. We have

$$\pi_{**}^{\mathbb{Q}_q}(HZ/2) \cong \begin{cases} \mathbb{Z}/2[\tau, \pi, u]/(\pi^2, u^2) & \text{if } q \equiv 1 \pmod{4}, \\ \mathbb{Z}/2[\tau, \pi, \rho]/(\rho^2, \rho\pi + \pi^2) & \text{if } q \equiv 3 \pmod{4} \end{cases}$$

where  $|\tau| = (0, -1)$ ,  $|\pi| = |u| = |\rho| = (-1, -1)$ . The homotopy groups of  $H\mathbb{Z}$  over  $\mathbb{Q}_q$ ,  $q$  odd, appear in [Orm11, Thm. 5.8]:

$$\pi_{**}^{\mathbb{Q}_q}(HZ) \cong \begin{cases} \mathbb{Z}\{1\} & \text{if } (*, *) = (0, 0), \\ \mathbb{Z}\{\pi\} \oplus \mathbb{Z}/2^{s_q(0)}\{x_q\} & \text{if } (*, *) = (-1, -1), \\ \mathbb{Z}/2^{s_q(0)}\{x_q \pi\} & \text{if } (*, *) = (-2, -2), \\ \mathbb{Z}/2^{s_q(i-1)}\{\pi^{\epsilon-1} x_q \tau^{i-1}\} & \text{if } (*, *) = (-\epsilon, -i + 1 - \epsilon), \ i \geq 2, \ \epsilon = 1 \text{ or } 2, \end{cases}$$

where  $x_q = u$  if  $q \equiv 1 \pmod{4}$  and  $x_q = \rho$  if  $q \equiv 3 \pmod{4}$ . Equivalently, there is an additive isomorphism

$$(3) \quad \pi_{**}^{\mathbb{Q}_q}(HZ) \cong \left( \mathbb{Z}\{1\} \oplus \bigoplus_{i \geq 0} \mathbb{Z}/2^{s_q(i)}\{x_q \tau^i\} \right) \otimes \mathbb{Z}[\pi]/(\pi^2) \cong \pi_{**}^{\mathbb{F}_q}(HZ) \otimes \mathbb{Z}[\pi]/(\pi^2);$$

if  $q \equiv 1 \pmod{4}$ , this is an isomorphism of graded rings.

2.2.4.  $\mathbb{Q}_2$ . These results appear in [OØ13]. We have

$$\pi_{**}^{\mathbb{Q}_2}(HZ/2) \cong \mathbb{Z}/2[\tau, \pi, u, \rho]/(\rho^3, u^2, \pi^2, \rho u, \rho\pi, \rho^2 + u\pi),$$

where  $|\tau| = (0, -1)$ ,  $|\pi| = |u| = |\rho| = (-1, -1)$ . The coefficients of  $H\mathbb{Z}$  over  $\mathbb{Q}_2$  appear in the proof of [OØ13, Thm. 3.19] as

$$\pi_{**}^{\mathbb{Q}_2}(HZ) \cong \begin{cases} \mathbb{Z}\{1\} & \text{if } (*, *) = (0, 0), \\ \mathbb{Z}\{u\} \oplus \mathbb{Z}\{\pi\} \oplus \mathbb{Z}/2\{\rho\} & \text{if } (*, *) = (-1, -1), \\ \mathbb{Z}\{y_m \tau^m\} \oplus \mathbb{Z}/2^{s_3(m)}\{z_m \tau^m\} & \text{if } (*, *) = (-1, -m - 1), \ m > 0, \\ \mathbb{Z}/2^{s_3(m)}\{\rho^2 \tau^m\} & \text{if } (*, *) = (-2, -m - 2), \ m \geq 0, \\ 0 & \text{otherwise.} \end{cases}$$

where  $y_m$  is  $u$  for  $m$  odd and  $\pi$  for  $m$  even, and  $z_m$  is  $\pi$  for  $m$  odd and  $\rho$  for  $m$  even.

2.2.5.  $\mathbb{R}$ . These results appear, for instance, in [Hil11]. We have

$$\pi_{**}^{\mathbb{R}}(HZ/2) \cong \mathbb{Z}/2[\tau, \rho], \quad \pi_{**}^{\mathbb{R}}(HZ) \cong \mathbb{Z}[\tau^2, \rho]/(2\rho).$$

2.2.6.  $\mathbb{Q}$ . These results appear in [OØ13, Sec. 5]. The groups  $\pi_{**}^{\mathbb{Q}}(H\mathbb{Z}/2)$  can be obtained from the mod two Milnor K-theory of  $\mathbb{Q}$  [OØ13, Prop. 5.3],

$$k_n^M(\mathbb{Q}) \cong \begin{cases} \mathbb{Z}/2\{1\} & \text{if } n = 0, \\ \mathbb{Z}/2\{\rho\} \oplus \bigoplus_{p \geq 2, \text{ prime}} \mathbb{Z}/2\{[p]\}, & \text{if } n = 1, \\ \mathbb{Z}/2\{\rho^2\} \oplus \bigoplus_{p \geq 3, \text{ prime}} \mathbb{Z}/2\{a_p\}, & \text{if } n = 2, \\ \mathbb{Z}/2\{\rho^n\} & \text{if } n \geq 3, \end{cases}$$

by tensoring with  $\mathbb{Z}/2[\tau]$ . The multiplicative structure and  $\rho$ -module structure is described further in [OØ13, Props. 5.3-5.4]. The Hasse map

$$k_*^M(\mathbb{Q}) \rightarrow \prod_v k_*^M(\mathbb{Q}_v)$$

sends pure symbols to their obvious images in  $\prod k_1^M(\mathbb{Q}_v)$ ,  $a_p$  to the unique nonzero class in  $k_2^M(\mathbb{Q}_p)$  and to 0 in  $k_2^M(\mathbb{Q}_\ell)$ ,  $\ell \neq p$ .

**Remark 2.4.** To simplify our comparison with  $\pi_{**}^{\mathbb{Q}}(H\mathbb{Z})$  and  $\pi_{**}^{\mathbb{Q}_\nu}(H\mathbb{Z}/2)$  in the sequel, we note that

$$\pi_{**}^{\mathbb{Q}}(H\mathbb{Z}/2) \cong \pi_{**}^{\mathbb{R}}(H\mathbb{Z}/2) \oplus \mathbb{Z}/2[\tau]\{[2]\} \oplus \bigoplus_{q \text{ odd}} \mathbb{Z}/2[\tau]\{[q], a_q\}.$$

The summand  $\pi_{**}^{\mathbb{R}}(H\mathbb{Z}/2)$  maps isomorphically onto  $\pi_{**}^{\mathbb{R}}(H\mathbb{Z}/2)$  under the map

$$\pi_{**}^{\mathbb{Q}}(H\mathbb{Z}/2) \rightarrow \pi_{**}^{\mathbb{R}}(H\mathbb{Z}/2),$$

and for each prime  $q$ , the elements  $[q]$  and  $a_q$  map to  $\pi$  and  $\pi x_q$ , respectively, under

$$\pi_{**}^{\mathbb{Q}}(H\mathbb{Z}/2) \rightarrow \pi_{**}^{\mathbb{Q}_q}(H\mathbb{Z}/2).$$

The groups  $\pi_{**}^{\mathbb{Q}}(H\mathbb{Z})$  are more complicated. Specializing [OØ13, Thm. 5.13] to the case  $n = 0$ , we have

$$\pi_{**}^{\mathbb{Q}}(H\mathbb{Z}) \cong A \oplus B \oplus C,$$

where  $A = \bigoplus_{p \equiv 3 \pmod{4}, \text{ prime}} A_p$  with  $A_p$  the bigraded abelian group defined by

$$(A_p)_{**} = \begin{cases} \mathbb{Z} & \text{if } (*, *) = (-1, -1), \\ \mathbb{Z}/2 & \text{if } (*, *) = (-2, -2r - 2), \ r \geq 0, \\ \mathbb{Z}/2^{s_p(2r+1)} & \text{if } (*, *) = (-2, -2r - 3), \ r \geq 0, \\ 0 & \text{otherwise,} \end{cases}$$

$B = \bigoplus_{p \equiv 1 \pmod{4}, \text{ prime}} B_p$ , with

$$(B_p)_{**} = \begin{cases} \mathbb{Z} & \text{if } (*, *) = (-1, -1), \\ \mathbb{Z}/2^{s_p(r)} & \text{if } (*, *) = (-2, -2 - r), \ r \geq 0, \\ 0 & \text{otherwise,} \end{cases}$$

and  $C = C'(0) \oplus C'''(0)$ , with

$$C'(0) = \mathbb{Z}_2[\rho, \tau^2]/(2\rho),$$

$$C'''(0)_{**} = \begin{cases} \mathbb{Z} & \text{if } (*, *) = (-1, -2r - 1), \ r \geq 0, \\ \mathbb{Z}/2^{3+\nu(r+1)} & \text{if } (*, *) = (-1, -2r - 2), \ r \geq 0, \\ 0 & \text{otherwise.} \end{cases}$$

**Remark 2.5.** The groups  $\pi_{**}^{\mathbb{Q}}(H\mathbb{Z})$  have an alternative description which will be useful in the sequel. Let

$$D_q := \begin{cases} A_q & \text{if } q \equiv 3 \pmod{4}, \\ B_q & \text{if } q \equiv 1 \pmod{4}, \end{cases}$$

so

$$\pi_{**}^{\mathbb{Q}}(H\mathbb{Z}) \cong C \oplus \bigoplus_{q \text{ odd}} D_q.$$

We have

$$(D_q)_{**} \cong \begin{cases} \pi_{**+1, **+1}^{\mathbb{F}_q}(H\mathbb{Z}) & \text{if } (*, *) \neq (0, 0), \\ 0 & \text{if } (*, *) = (0, 0). \end{cases}$$

Here,  $\pi_{**+1, **+1}^{\mathbb{F}_q}(H\mathbb{Z})$  is shorthand for the  $\pi$ -divisible part of  $\pi_{**}^{\mathbb{Q}_q}(H\mathbb{Z})$ , cf. (3). Moreover, we observe that the summands  $C'(0)$  and  $C'''(0)$  of  $C$  can be identified with familiar objects:

$$C'(0) \cong \pi_{**}^{\mathbb{R}}(H\mathbb{Z}),$$

and there is an obvious inclusion

$$C'''(0) \hookrightarrow \pi_{**}^{\mathbb{Q}_2}(H\mathbb{Z})$$

with image those subgroups generated by classes of the form  $\pi\tau^m$ ,  $m \geq 0$ .

[OØ13, Sec. 5] implies that all of these identifications are realized via the maps

$$\pi_{**}^{\mathbb{Q}}(H\mathbb{Z}) \rightarrow \pi_{**}^{\mathbb{Q}_\nu}(H\mathbb{Z}),$$

where  $\mathbb{Q}_\nu$  ranges over all places.

### 3. COEFFICIENT RINGS OF $H\mathbb{Z}/2^n$

In Section 5, we will see that the slices of  $L$  are comprised of suspensions of the Eilenberg–MacLane spectra  $H\mathbb{Z}/2^n$  for various  $1 \leq n \leq \infty$ . In this section, we record the coefficients of these spectra over our fields of interest.

The motivic Adams spectral sequence [DI10] for  $H\mathbb{Z}$  has the following form.

$$E_1^{s,w,t} = \pi_{t-s,w}(H\mathbb{Z}/2)[h_0] \implies \pi_{t-s,w}H\mathbb{Z}.$$

Here we use the Adams grading; the element  $h_0$  has degree  $(s, w, t) = (1, 0, 1)$ . The abutment is known, and this information determines the differentials (see [Ky15] for  $F = \mathbb{F}_q$  and [OØ13] for  $F = \mathbb{Q}_q, \mathbb{Q}$ ).

Similarly, we have the motivic Adams spectral sequence for  $H\mathbb{Z}/2^n$ :

$$(4) \quad E_1^{s,w,t} = \pi_{t-s,w}(H\mathbb{Z}/2)[h_0]/h_0^n \implies \pi_{t-s,w}(H\mathbb{Z}/2^n).$$

The differentials can be recovered from the motivic Adams spectral sequence for  $H\mathbb{Z}$ .

**Remark 3.1.** Over algebraically closed fields and over the real numbers, we can compute  $\pi_{**}^F(H\mathbb{Z}/2^n)$  directly using the long exact sequence in homotopy associated to the cofiber sequence

$$H\mathbb{Z} \xrightarrow{\cdot 2^n} H\mathbb{Z} \rightarrow H\mathbb{Z}/2^n.$$

We have

$$\pi_{**}^{\bar{F}}(H\mathbb{Z}/2^n) \cong \mathbb{Z}/2^n[\tau] \quad \text{and} \quad \pi_{**}^{\mathbb{R}}(H\mathbb{Z}/2^n) \cong \mathbb{Z}/2^n[\tau^2, \rho]/(2\rho).$$

**Proposition 3.2.** *The differentials in the  $F$ -motivic Adams spectral sequence for  $H\mathbb{Z}/2^n$  are determined via the Leibniz rule by the following ( $i \geq 1$ ):*

(1) When  $F = \mathbb{F}_q$ :

$$d_{s_q(i-1)}\tau^i = x_q\tau^{i-1}h_0^{s_q(i-1)}, \quad s_q(i-1) < n,$$

where  $x_q = u$  if  $q \equiv 1 \pmod{4}$  and  $x_q = \rho$  if  $q \equiv 3 \pmod{4}$ .

(2) When  $F = \mathbb{Q}_q$ :

$$d_{s_q(i-1)}\tau^i = x_q\tau^{i-1}h_0^{s_q(i-1)}, \quad s_q(i-1) < n,$$

where  $x_q = u$  if  $q \equiv 1 \pmod{4}$  and  $x_q = \rho$  if  $q \equiv 3 \pmod{4}$ .

(3) When  $F = \mathbb{Q}_2$ :

$$d_1\tau = \rho h_0, \quad d_{3+\nu(i)}\tau^{2i} = \pi\tau^{2i-1}h_0^{3+\nu(i)}, \quad \nu(i) < n-3.$$

(4) When  $F = \mathbb{Q}$ :

$$d_1\tau = \rho h_0, \quad d_1[p]\tau = (\rho^2 + a_p)h_0 \quad p \equiv 3 \pmod{4},$$

$$d_{s_p(i-1)}[p]\tau^i = a_p\tau^{i-1}h_0^{s_p(i-1)}, \quad 1 \leq s_p(i-1) < n \text{ and } i \text{ even for } p \equiv 3 \pmod{4},$$

$$d_{3+\nu(i)}\tau^{2i}h_0 = [2]\tau^{2i-1}h_0^{4+\nu(i)}, \quad \text{with } \nu(i) < n-3.$$

*Proof.* (1) This follows from [Kyl15, Lem. 4.2.1, Lem. 4.2.2].<sup>4</sup>

(2) This follows from [OØ13, Thm. 3.16, Thm. 3.17].

(3) This follows from [OØ13, Thm. 3.18, Thm. 3.19].

(4) This follows from [OØ13, Thm. 5.5, Thm. 5.8].

□

**Proposition 3.3.** *The coefficient rings of  $H\mathbb{Z}/2^n$ ,  $1 \leq n < \infty$ , are given by the following formulas. In cases (1) and (2), we write  $i(w)$  for  $\min(s_q(w-1), n)$ .*

(1) When  $F = \mathbb{F}_q$  with  $q \equiv 1 \pmod{4}$ :

$$\pi_{s,w}^{\mathbb{F}_q} H\mathbb{Z}/2^n = \begin{cases} \mathbb{Z}/2^n\{1\} & \text{if } s = 0, w = 0, \\ \mathbb{Z}/2^{i(-w)}\{2^{n-i(-w)}\tau^{-w}\} & \text{if } s = 0, w \leq -1, \\ \mathbb{Z}/2^{i(-w)}\{\tau^{-1-w}x_q\} & \text{if } s = -1, w \leq -1, \\ 0 & \text{otherwise.} \end{cases}$$

Here  $x_q = u$  if  $q \equiv 1 \pmod{4}$  and  $x_q = \rho$  if  $q \equiv 3 \pmod{4}$ .

(2) When  $F = \mathbb{Q}_q$  with  $q \equiv 1 \pmod{4}$ :

$$\pi_{s,w}^{\mathbb{Q}_q} H\mathbb{Z}/2^n = \begin{cases} \mathbb{Z}/2^{i(-w)}\{2^{n-i(-w)}\tau^{-w}\} & \text{if } s = 0, w \leq 0, \\ \mathbb{Z}/2^{i(-w)}\{\tau^{-1-w}x_q\} \oplus \mathbb{Z}/2^{i(-w-1)}\{2^{n-i(-w-1)}\tau^{-1-w}\pi\} & \text{if } s = -1, w \leq -1 \\ \mathbb{Z}/2^{i(-w-1)}\{\tau^{-2-w}\pi x_q\} & \text{if } s = -2, w \leq -2 \\ 0 & \text{otherwise,} \end{cases}$$

<sup>4</sup>Note that for  $q \equiv 3 \pmod{4}$ , the exponent of  $h_0$  in the target is off by one in *loc. cit.*

(3) When  $F = \mathbb{Q}_2$ :

$$\pi_{s,w}^{\mathbb{Q}_2}(H\mathbb{Z}/2^n) \cong \begin{cases} \mathbb{Z}/2^{i(-w)}\{2^{n-i(-w)}\tau^{-w}\} & \text{if } s = 0, w \leq 0, \\ \mathbb{Z}/2^n\{\tau^{-1-w}u\} \oplus \mathbb{Z}/2^{i(-w)}\{2^{n-i(-w)}\tau^{-1-w}\pi\} & \\ \oplus \mathbb{Z}/2\{2^{n-1}\tau^{-1-w}\rho\} & \text{if } s = -1, w \leq -2 \text{ even}, \\ \mathbb{Z}/2^{i(-1-w)}\{2^{n-i(-1-w)}\tau^{-1-w}u\} \oplus \mathbb{Z}/2^n\{\tau^{-1-w}\pi\} & \\ \oplus \mathbb{Z}/2\{\tau^{-1-w}\rho\} & \text{if } s = -1, w \leq -1 \text{ odd}, \\ \mathbb{Z}/2^{i(-w-1)}\{2^{n-i(-w-1)}\tau^{-2-w}\rho^2\} & \text{if } s = -2, w \leq -1, \\ 0 & \text{otherwise,} \end{cases}$$

where  $i(w) = 1$  when  $w$  is odd and  $\min(2 + \nu(w), n)$  when  $w$  is even.

(4) When  $F = \mathbb{Q}$ :

$$\pi_{**}^{\mathbb{Q}}(H\mathbb{Z}/2^n) \cong C'''_{**}(0) \oplus C'_{**}(0) \oplus \bigoplus_{q \text{ odd}} D_q(n),$$

where

$$(D_q(n))_{**} \cong \begin{cases} \pi_{**+1, **+1}^{\mathbb{F}_q}(H\mathbb{Z}/2^n) & \text{if } (*, *) \neq (0, 0), \\ 0 & \text{if } (*, *) = (0, 0), \end{cases}$$

$$C'_{**}(0) \cong \pi_{**}^{\mathbb{R}}(H\mathbb{Z}/2^n),$$

and

$$C'''(0) \hookrightarrow \pi_{**}^{\mathbb{Q}_2}(H\mathbb{Z}/2^n)$$

can be identified with the subgroups generated by classes of the form  $\pi\tau^m$ ,  $m \geq 0$ .

Here,  $\pi_{**+1, **+1}^{\mathbb{F}_q}$  is shorthand for the  $\pi$ -divisible part of  $\pi_{**}^{\mathbb{Q}_q}$ .

*Proof.* The results follow from the motivic Adams spectral sequence in (4) and differentials in Proposition 3.2.  $\square$

#### 4. COEFFICIENT RINGS OF $kq$

Recall the slices for  $kq$  in Equation (1). In this section, we describe the effective slice spectral sequence for  $kq$  over various base fields.

**4.1. Algebraically closed fields.** Let  $F = \bar{F}$  be an algebraically closed field. The effective slice spectral sequence for  $kq$  over  $F$  was computed in [BIK22, Sec. 3]. The  $E_1$ -term of the ESSS is depicted in Figure 2.

The differential  $d_1(v_1^2) = \tau h_1^3$  follows by Betti realization [BIK22, Prop. 3.2], with all remaining differentials following by the Leibniz rule. The spectral sequence collapses at  $E_2$ ; the resulting  $E_\infty$ -page is depicted in Figure 3.

**4.2. Finite fields.** The  $E_1$ -page of the ESSS over  $\mathbb{F}_q$  can be obtained from the  $E_1$ -page of the ESSS over algebraically closed fields (Figure 2) by letting a rectangle denote  $\mathbb{Z}$  instead of  $\mathbb{Z}[\tau]$ , and then juxtaposing a copy of the  $E_1$ -page, shifted by  $(-1, 1)$ , with each rectangle replaced by a diamond denoting the  $u$ - or  $\rho$ -divisible part  $\pi_{**}^{\mathbb{F}_q}(H\mathbb{Z})$ . The resulting  $E_1$ -page is depicted in Figure 4.

The differential  $d_1(v_1^2) = \tau h_1^3$  follows from base change to the algebraic closure, and all remaining differentials follow by the Leibniz rule. The resulting pattern of  $d_1$ -differentials is depicted in Figure 4.

The ESSS collapses for degree reasons at  $E_2$ . The  $E_\infty$ -page is shown in Figure 5. The hidden extensions  $h \cdot 2v_1^{2+4k}u = \tau^2 h_1^3 v_1^{4k}$ ,  $k \geq 0$ , follow by comparison to Kylling's computation of  $\pi_{**}^{\mathbb{F}_q}(kq)$  via the motivic Adams spectral sequence [Kyl15, Sec. 4].

**4.3.  $\mathbb{Q}_q$  with  $q$  odd.** The  $E_1$ -page of the ESSS over  $\mathbb{Q}_q$  can be obtained from the  $E_1$ -page of the ESSS over  $\mathbb{F}_q$  using the additive isomorphism (3), which implies that there is an additive isomorphism

$$E_1^{\mathbb{Q}_q}(kq) \cong E_1^{\mathbb{F}_q}(kq) \otimes \mathbb{Z}[\pi]/(\pi^2),$$

where  $|\pi| = (-1, 0, -1)$ . Graphically, this means the  $E_1$ -term over  $\mathbb{Q}_q$  consists of two copies of the  $E_1$ -page over  $\mathbb{F}_q$ : one copy as it appears in Figure 4, and one copy shifted by  $(-1, 1)$ . The result is depicted in Figure 6.

As in the case of finite fields, all  $d_1$ -differentials follow from base change to the algebraic closure and  $\pi^\delta x_q^\epsilon \tau^n$ -linearity for the appropriate choices of  $\delta, \epsilon \in \{0, 1\}$ . The resulting  $E_\infty$ -page is identical to the  $E_\infty$ -page over  $\mathbb{F}_q$ , tensored with  $\mathbb{Z}[\pi]/(\pi^2)$ . Hidden extensions follow from similar arguments. The resulting groups are depicted in Figure 7.

**4.4.  $\mathbb{Q}_2$ .** Since  $\rho^2$  is non-zero over  $\mathbb{Q}_2$ , the ESSS over  $\mathbb{Q}_2$  has a different  $d_1$ -differential pattern. The  $d_1$ -differentials in the ESSS for  $KQ$  (and consequently,  $kq$ ) were computed in terms of Steenrod operations in [RØ16, Thm. 5.5]. The  $E_1$ -term is depicted in Figure 8.

In Figure 8, the red differentials are given by taking  $Sq^2$ , and the brown differentials are given by multiplying by  $\tau$ .

**Example 4.1.** We explain the  $d_1$  calculation by way of example.

- (1) There is a red differential between the class  $\mathbb{Z}/2[\tau]\{h_1\}$  at  $(1, 1)$  and the class  $\mathbb{Z}/2[\tau]\{h_1^2 \rho^2\}$  at  $(0, 4)$ . The formula for the differential is

$$d_1(\tau^{4n+2}h_1) = \tau^{4n+1}\rho^2 h_1^2 \text{ and } d_1(\tau^{4n+3}h_1) = \tau^{4n+2}\rho^2 h_1^2, n \geq 0.$$

Therefore, on the  $E_2$ -page, we have a  $\mathbb{Z}/2\{1, \tau^3\}[\tau^4]$  in the degree of the target and a  $\mathbb{Z}/2\{1, \tau\}[\tau^4]$  in the degree of the source.

- (2) There is a brown differential between the class  $\pi_{-2,*}^{\mathbb{Q}_2}(H\mathbb{Z})\{v_1^2\}$  at  $(2, 2)$  and the class  $\mathbb{Z}/2[\tau]\{\rho^2 h_1^3\}$  at  $(1, 5)$ . The formula for the differential is

$$d_1(\tau^n \rho^2 v_1^2) = \tau^{n+1} \rho^2 h_1^3, n \geq 0.$$

Therefore, on the  $E_2$ -page, we have a  $\mathbb{Z}/2$  in the degree of the target. The surviving group in the degree of the source is obtained from  $\pi_{-2,*}^{\mathbb{Q}_2}(H\mathbb{Z})$  by decreasing the order of 2-torsion by exactly 1 in each weight (thus is trivial in even weights).

- (3) In the case of (2), the classes in  $\mathbb{Z}/2[\tau]\{h_1^2\}$  at  $(2, 2)$  also support red differentials to the classes in  $\mathbb{Z}/2[\tau]\{\rho^2 h_1^3\}$  at  $(1, 5)$ . Using the differential formulas, we see that the following linear combinations of the source classes survive:

$$\tau^{4n+2}h_1^2 + \tau^{4n}\rho^2 v_1^2 \quad \text{and} \quad \tau^{4n+3}h_1^2 + \tau^{4n+1}\rho^2 v_1^2, \quad n \geq 0.$$

The  $E_2$ -page is depicted in Figure 9. There are no room for  $d_2$ -differentials, therefore we have  $E_2 = E_\infty$ .

4.5.  $\mathbb{R}$ . The ESSS for  $kq$  over  $\mathbb{R}$  is the subject of [BIK22, Sec. 4]. There are two interesting differentials over  $\mathbb{R}$  [BIK22, Prop. 5.2]:

$$d_1(v_1^2) = \tau h_1^3, \quad d_1(\tau^2) = \rho^2 \tau h_1.$$

The  $E_1$ -page is depicted in [BIK22, Fig. 5], and the  $E_\infty$ -page is depicted in [BIK22, Figs. 6-8].

4.6.  $\mathbb{Q}$ . We will now analyze the ESSS for  $kq$  over  $\mathbb{Q}$ . To begin, recall the presentations of  $\pi_{**}^{\mathbb{Q}}(H\mathbb{Z}/2)$  and  $\pi_{**}^{\mathbb{Q}}(H\mathbb{Z})$  from Remark 2.4 and Remark 2.5. Since  $E_1^{\mathbb{Q}}(kq)$  is comprised of shifts of these groups, it naturally decomposes as

$$E_1^{\mathbb{Q}}(kq) \cong E_1^+(kq) \oplus E_1^-(kq),$$

where  $E_1^+(kq) \subseteq E_1^{\mathbb{Q}}(kq)$  is obtained by making the replacements

$$\pi_{**}^{\mathbb{Q}}(H\mathbb{Z}/2) \rightsquigarrow \bigoplus_{q \text{ odd}} \mathbb{Z}/2[\tau]\{[q], a_q\}, \quad \pi_{**}^{\mathbb{Q}}(H\mathbb{Z}) \rightsquigarrow \bigoplus_{q \text{ odd}} D_q,$$

and  $E_1^-(kq) \subseteq E_1^{\mathbb{Q}}(kq)$  is obtained by making the replacements

$$\pi_{**}^{\mathbb{Q}}(H\mathbb{Z}/2) \rightsquigarrow \pi_{**}^{\mathbb{R}}(H\mathbb{Z}/2) \oplus \mathbb{Z}/2[\tau]\{[2]\}, \quad \pi_{**}^{\mathbb{Q}}(H\mathbb{Z}) \rightsquigarrow C \cong \pi_{**}^{\mathbb{R}}(H\mathbb{Z}) \oplus C'''(0).$$

Graphically, we can obtain  $E_1^{\mathbb{Q}}(kq)$  from  $E_1^{\mathbb{R}}(kq)$  (Figure 2) by replacing each bullet by a copy of  $\pi_{**}^{\mathbb{Q}}(H\mathbb{Z}/2)$  and replacing each square by a copy of  $\pi_{**}^{\mathbb{Q}}(H\mathbb{Z})$ ; the replacements are shown in Figure 10.

The purpose of this decomposition is to understand the map

$$E_1^{\mathbb{Q}}(kq) \rightarrow E_1^{\mathbb{Q}\nu}(kq)$$

for each place  $\nu$  of  $\mathbb{Q}$ . In particular, we see that the Hasse map

$$E_1^{\mathbb{Q}}(kq) \rightarrow \prod_{\nu} E_1^{\mathbb{Q}\nu}(kq)$$

is injective. It follows that the nontrivial  $d_1$ -differentials over  $\mathbb{Q}$  are generated by

$$d_1([q]\tau^i v_1^{2k}) = [q]\tau^{i+1} h_1^3 v_1^{2k-2}, \quad d_1(a_{q'}\tau^i v_1^{2k}) = a_{q'}\tau^{i+1} h_1^3 v_1^{2k-2}, \quad d_1(\tau^2) = \rho^2 \tau h_1,$$

where  $q$  ranges over all primes,  $q'$  ranges over all odd primes, and  $i$  and  $k$  range over all nonnegative integers. Note that none of the more exotic differentials (red ones in Figure 8) from the  $\mathbb{Q}_2$ -case lift to  $\mathbb{Q}$  since the sources and targets do not lift to  $\mathbb{Q}$ .

There is no room for longer differentials, so  $E_2^{\mathbb{Q}}(kq) \cong E_\infty^{\mathbb{Q}}(kq)$ . All hidden extensions can be handled by comparison with the local places.

**Remark 4.2.** Our description of the  $E_1$ -term over  $\mathbb{Q}$  makes clear that the map

$$E_1^{\mathbb{Q}}(kq) \rightarrow \prod_{\nu} E_1^{\mathbb{Q}\nu}(kq)$$

is injective. Since all of the differentials over  $\mathbb{Q}$  are lifted from differentials over the local places, we conclude that the Hasse map

$$\pi_{**}^{\mathbb{Q}}(kq) \rightarrow \prod_{\nu} \pi_{**}^{\mathbb{Q}\nu}(kq)$$

is injective, i.e.,  $kq$  satisfies the motivic Hasse principle in the sense of [OØ13, Sec. 4],

5. COEFFICIENT RINGS OF  $L$  OVER PRIME FIELDS

In this section, we describe the effective slice spectral sequence for  $L$  over various base fields.

**5.1. Algebraically closed fields.** The ESSS for  $L$  over algebraically closed fields was computed in [BIK22, Sec. 3]. The multiplicative generators of the  $E_1$ -term appear in [BIK22, Table 3] and the  $E_1$ -term is shown in [BIK22, Fig. 3]. The  $d_1$ -differentials appear in [BIK22, Table 4] and the resulting  $E_2 = E_\infty$ -page appears in [BIK22, Fig. 4]. Hidden extensions are handled in [BIK22, Prop. 3.16].

For ease of reference, we have reproduced [BIK22, Fig. 3] and [BIK22, Fig. 4] in Figure 11 and Figure 12, respectively.

**5.2. Finite fields.** To compute the  $E_1$ -term of the ESSS for  $L$  over finite fields, we must analyze the effect of  $\psi^3 - 1$  on the slices of  $kq$ . Comparison with the algebraically closed case implies that the only possible nontrivial action of  $\psi^3 - 1$  is on the integer slices, i.e.,

$$\psi^3 - 1 : \pi_{**}^{\mathbb{F}_q}(H\mathbb{Z})\{v_1^{2k}\} \rightarrow \pi_{**}^{\mathbb{F}_q}(H\mathbb{Z})\{v_1^{2k}\},$$

which may be identified with

$$\cdot 2^{\nu(3^{2k}-1)} = \cdot 2^{\nu(k)+3} : \pi_{**}^{\mathbb{F}_q}(H\mathbb{Z})\{v_1^{2k}\} \rightarrow \pi_{**}^{\mathbb{F}_q}(H\mathbb{Z})\{v_1^{2k}\}.$$

Recalling the functions  $s_q(i)$  and notation  $x_q$  from Definition 2.3, we may write this more explicitly as

$$\cdot 2^{\nu(k)+3} : \mathbb{Z}\{v_1^{2k}\} \oplus \bigoplus_{i \geq 0} \mathbb{Z}/2^{s_q(i)}\{v_1^{2k}x_q\tau^i\}.$$

The kernel and cokernel of

$$\cdot 2^{\nu(k)+3} : \mathbb{Z}\{v_1^{2k}\} \rightarrow \mathbb{Z}\{v_1^{2k}\}$$

are 0 and  $\mathbb{Z}/2^{\nu(k)+3}$ , respectively. On the components indexed by  $x_qv_1^{2k}\tau^i$ ,

$$\cdot 2^{\nu(k)+3} : \mathbb{Z}/2^{s_q(i)}\{x_qv_1^{2k}\tau^i\} \rightarrow \mathbb{Z}/2^{s_q(i)}\{x_qv_1^{2k}\tau^i\},$$

we have

$$\ker \cong \begin{cases} \mathbb{Z}/2^{s_q(i)}\{x_qv_1^{2k}\tau^i\} & \text{if } s_q(i) \leq \nu(k) + 3, \\ \mathbb{Z}/2^{\nu(k)+3}\{2^{s_q(i)-\nu(k)-3}x_qv_1^{2k}\tau^i\} & \text{if } s_q(i) > \nu(k) + 3, \end{cases}$$

and

$$\text{coker} \cong \begin{cases} \mathbb{Z}/2^{s_q(i)}\{x_qv_1^{2k}\tau^i\} & \text{if } s_q(i) \leq \nu(k) + 3, \\ \mathbb{Z}/2^{s_q(i)-\nu(k)-3}\{x_qv_1^{2k}\tau^i\} & \text{if } s_q(i) > \nu(k) + 3. \end{cases}$$

**Definition 5.1.** For each  $k \geq 0$ , we define graded groups  $K_q(k)$  and  $C_q(k)$  as follows. Let

$$K_q(0) = C_q(0) := \pi_{-1,*}^{\mathbb{F}_q}(H\mathbb{Z})$$

denote the  $x_q$ -divisible part of  $\pi_{**}^{\mathbb{F}_q}(H\mathbb{Z})$ . For all  $k \geq 1$ , let

$$K_q(k) := \bigoplus_{i \geq 0} \ker(\cdot 2^{\nu(k)+3} : \mathbb{Z}/2^{s_q(i)}\{x_qv_1^{2k}\tau^i\} \rightarrow \mathbb{Z}/2^{s_q(i)}\{x_qv_1^{2k}\tau^i\}),$$

$$C_q(k) := \bigoplus_{i \geq 0} \text{coker}(\cdot 2^{\nu(k)+3} : \mathbb{Z}/2^{s_q(i)}\{x_qv_1^{2k}\tau^i\} \rightarrow \mathbb{Z}/2^{s_q(i)}\{x_qv_1^{2k}\tau^i\})$$

be the sums of the kernels and cokernels, respectively, described above.

Let  $\tilde{K}_q(k)$  denote the groups obtained from  $K_q(k)$  as follows. If  $k$  is even, then  $\tilde{K}_q(k) := K_q(k)$ . If  $k$  is odd, then:

- (1) If  $s_q(i) \leq \nu(k) + 3$ , then the  $i$ -th summand of  $\tilde{K}_q(k)$  is the group obtained from the  $i$ -th summand of  $K_q(k)$  by decreasing the order of 2-torsion by exactly 1 in each summand.
- (2) If  $s_q(i) > \nu(k) + 3$ , the  $i$ -th summand of  $\tilde{K}_q(k)$  is the same as the  $i$ -th summand in  $K_q(k)$ .

Let  $\tilde{C}_q(k)$  denote the groups obtained from  $C_q(k)$  as follows. If  $k$  is even, then  $\tilde{C}_q(k) := C_q(k)$ . If  $k$  is odd, then  $\tilde{C}_q(k)$  is obtained by decreasing the order of 2-torsion by exactly 1 in each summand of  $C_q(k)$ .

Definition 5.1 allows us to concisely describe the  $E_1$ - and  $E_\infty$ -terms of the ESSS for  $L$  in chart form. The  $E_1$ -term is depicted in Figure 13.

All of the differentials follow from base change to the algebraic closure and  $x_q$ -linearity of the  $d_1$ -differentials. Since  $s_q(i) \geq 1$  for all  $i \geq 0$ , the effect of each *nontrivial* differential is easy to describe: simply reduce the order of 2-torsion in the source and target by 2. However, describing which differentials are nontrivial is somewhat subtle.

The red differentials out of the dark green boxes (i.e., out of  $\mathbb{Z}/2^? \{ \iota \tau^i v_1^{2k} \}$ ) and dark green left-pointing triangles (i.e., out of  $C_q(k)$ ) are nontrivial for all  $i \geq 0$ , but the green differentials out of the right-pointing triangles (i.e., out of  $K_q(k)$ ) are trivial on some summands. Recall that the generator of the  $i$ -th summand in  $K_q(k)$  for  $k$  odd is

$$\begin{cases} x_q v_1^{2k} \tau^i & \text{if } s_q(i) \leq 3, \\ 2^{s_q(i) - \nu(k) - 3} x_q v_1^{2k} \tau^i & \text{if } s_q(i) > 3. \end{cases}$$

Here, we have used that  $\nu(k) = 0$  if  $k$  is odd to rewrite  $\nu(k) + 3$  as 3.

If  $s_q(i) \leq 3$ , then there is a differential

$$d_1(x_q v_1^{2k} \tau^i) = x_q h_1^3 v_1^{2k-2} \tau^{i+1},$$

but if  $s_q(i) > \nu(k) + 3$ , then we must have

$$d_1(2^{s_q(i) - \nu(k) - 3} x_q v_1^{2k} \tau^i) = 0$$

since

$$d_1(2^{s_q(i) - \nu(k) - 3} v_1^{2k}) = 0$$

by base change to the algebraic closure.

**Remark 5.2.** In practice, it is straightforward to determine on which summands the green differentials are nontrivial for a given  $q$ . For instance, if  $q = 3$ , then:

- If  $i \not\equiv 3 \pmod{4}$ , then  $s_3(i) \leq 3$ . Indeed, if  $i$  is even, then  $s_3(i) = 1 \leq 3$ , and if  $i \equiv 1 \pmod{4}$ , then  $s_3(i) = \nu(3^2 - 1) + \nu(i + 1) - 1 = 2 + \nu(i + 1) = 3 \leq 3$ .
- If  $i \equiv 3 \pmod{4}$ , then  $s_3(i) = \nu(3^2 - 1) + \nu(i + 1) - 1 = 2 + \nu(i + 1) > 3$ .

This leads us to the  $E_2$ -term. There is no room for higher differentials, so  $E_2 = E_\infty$ . All hidden extensions follow from comparison to the algebraic closure or  $\tau^n x_q$ -linearity. The resulting groups are depicted in Figure 14.

**5.3.  $\mathbb{Q}_q$  with  $q$  odd.** As with  $kq$  (Section 4.3), the computation of  $\pi_{**}^{\mathbb{Q}_q}(L)$  for  $q$  odd follows from the analogous computation over  $\mathbb{F}_q$  (Section 5.2). The additive isomorphism (3) implies that

$$E_1^{\mathbb{Q}_q}(L) \cong E_1^{\mathbb{F}_q}(L) \otimes \mathbb{Z}[\pi]/(\pi^2).$$

Thus the  $E_1$ -term over  $\mathbb{Q}_q$  can be obtained from Figure 13 by superimposing an identical copy shifted by  $(-1, 1)$ . Moreover, the  $d_1$ -differentials occur in both copies; this follows as usual from base change to the algebraic closure and  $\pi^\delta x^\epsilon \tau^n$ -linearity for the appropriate choices of  $n \geq 0$  and  $\delta, \epsilon \in \{0, 1\}$ .

There is no room for further differentials, so  $E_2 = E_\infty$ . By the above discussion, the  $E_\infty$ -term satisfies

$$E_\infty^{\mathbb{Q}_q}(L) \cong E_\infty^{\mathbb{F}_q}(L) \otimes \mathbb{Z}[\pi]/(\pi^2),$$

so it can be obtained from Figure 14 by superimposing the same picture shifted by  $(-1, 1)$ .

5.4.  $\mathbb{Q}_2$ . As in §5.2, we calculate the kernels and cokernels of the reduced Adams operation.

**Definition 5.3.** For all  $k \geq 1$ , let

$$K_2(k)\{x\} := \bigoplus_{i \geq 0} \ker(\cdot 2^{\nu(k)+3} : \mathbb{Z}/2^{s_3(i)}\{xv_1^{2k}\tau^i\} \rightarrow \mathbb{Z}/2^{s_3(i)}\{xv_1^{2k}\tau^i\})$$

$$C_2(k)\{x\} := \bigoplus_{i \geq 0} \operatorname{coker}(\cdot 2^{\nu(k)+3} : \mathbb{Z}/2^{s_3(i)}\{xv_1^{2k}\tau^i\} \rightarrow \mathbb{Z}/2^{s_3(i)}\{xv_1^{2k}\tau^i\})$$

be the sums of kernels and cokernels, respectively, for  $x$  being either  $z_i$ ,  $y_i$ , or  $\rho^2$ .

Define  $K_2(0) = C_2(0)$  to be  $\pi_{-2,*}^{\mathbb{Q}_2}(H\mathbb{Z})$ , and define  $\underline{K}_2(0)$  to be  $\pi_{-1,*}^{\mathbb{Q}_2}(H\mathbb{Z})$ .

We define  $\underline{C}_2(k)$ ,  $k \geq 0$  to be the sum

$$\underline{C}_2(k) := C_2(k)\{z_i\} \oplus \bigoplus_{i \geq 0} \mathbb{Z}/2^{\nu(k)+3}\{y_i\tau^i\} \oplus \mathbb{Z}/2^{\nu(k)+3}\{u\}.$$

Let  $\tilde{K}_2(k)$  denote the groups obtained from  $K_2(k)$  by decreasing the order of 2-torsion by exactly 1 in each summand except the  $(4i - 1)$ -th summand for all positive integer  $i$ .

Let  $\tilde{C}_2(k)$  denote the groups obtained from  $C_2(k)$  by decreasing the order of 2-torsion by exactly 1 in each summand; similar for  $\underline{\tilde{C}}_2(k)$

We use Definition 5.3 to describe the  $E_1$ -term and  $E_\infty$ -term of the ESSS for  $L$ . The  $E_1$ -term is depicted in Figure 15.

In Figure 15, the red differentials are given by taking  $Sq^2$ , and the brown differentials are given by multiplying by  $\tau$ . The calculation is similar to the case for  $kq$  in §4.4. The  $E_2$ -page is depicted in Figure 16.

Every potential higher differential hits an  $\eta$ -periodic class, or is from the unit 1. By comparing with the  $\eta$ -inverted result in [Wil18, Cor. 11], there is no possibility for nontrivial higher differentials. Therefore, over  $\mathbb{Q}_2$ , the ESSS for  $L$  collapses at  $E_2$ .

5.5.  $\mathbb{R}$ . The ESSS for  $L$  over  $\mathbb{R}$  was computed in [BIK22, Sec. 5]. The multiplicative generators of the  $E_1$ -term appear in [BIK22, Table 8] and the  $E_1$ -term is depicted in [BIK22, Fig. 10]. The values of the  $d_1$ -differentials on the multiplicative generators appear in [BIK22, Table 10], and these values determine all of the  $d_1$ -differentials using the Leibniz rule in conjunction with the relations recorded in [BIK22, Table 9]. The higher differentials are described in [BIK22, Prop. 5.11]. The resulting  $E_\infty$ -page is depicted in [BIK22, Figs. 13-19].

5.6.  $\mathbb{Q}$ . To compute  $E_1^{\mathbb{Q}}(L)$ , we break it into four manageable pieces. First, there is a decomposition

$$E_1^{\mathbb{Q}}(L) \cong K^{\mathbb{Q}}(L) \oplus \Sigma^{-1}C^{\mathbb{Q}}(L),$$

where  $K^{\mathbb{Q}}(L)$  is the kernel of  $\psi^3 - 1$  and  $C^{\mathbb{Q}}(L)$  is the cokernel of  $\psi^3 - 1$ . There are further decompositions

$$\begin{aligned} K^{\mathbb{Q}}(L) &\cong K^+(L) \oplus K^-(L), \\ C^{\mathbb{Q}}(L) &\cong C^+(L) \oplus C^-(L), \end{aligned}$$

where

$$\begin{aligned} K^+(L) &:= \ker(\psi^3 - 1 : E_1^+(kq) \rightarrow E_1^+(kq)), \\ K^-(L) &:= \ker(\psi^3 - 1 : E_1^-(kq) \rightarrow E_1^-(kq)), \\ C^+(L) &:= \text{coker}(\psi^3 - 1 : E_1^+(kq) \rightarrow E_1^+(kq)), \\ C^-(L) &:= \text{coker}(\psi^3 - 1 : E_1^-(kq) \rightarrow E_1^-(kq)). \end{aligned}$$

Here,  $E_1^+(kq)$  and  $E_1^-(kq)$  were defined in Section 4.6. We then have

$$E_1^{\mathbb{Q}}(L) \cong K^+(L) \oplus K^-(L) \oplus \Sigma^{-1}C^+(L) \oplus \Sigma^{-1}C^-(L).$$

Since  $E_1^+(kq)$  can be expressed entirely in terms of  $E_1^{\mathbb{F}^q}(kq)$ ,  $q$  odd, the groups  $K^+(L)$  and  $C^+(L)$  can be described using the computations from Section 5.2. More precisely,  $K^+(L) \oplus \Sigma^{-1}C^+(L)$  is obtained graphically by taking the sum over all odd primes of Figure 13, then shifting the entire picture by  $(-1, 1)$ .

The computation of  $K^-(L)$  and  $C^-(L)$  also largely follows from previous computations. Since  $E_1^{\mathbb{R}}(kq)$  is a summand of  $E_1^-(kq)$ , the kernel and cokernel of  $\psi^3 - 1$  over  $\mathbb{R}$  are summands in  $K^-(L) \oplus \Sigma^{-1}C^-(L)$ ; the relevant groups are depicted graphically in [BIK22, Fig. 10]. The complementary summand of  $E_1^-(kq)$  is obtained by replacing  $\pi_{**}(H\mathbb{Z})$  by  $C'''(0)$  and  $\pi_{**}(H\mathbb{Z}/2)$  by  $\mathbb{Z}/2[\tau]\{[2]\}$ . Since  $\psi^3 - 1$  is necessarily trivial on  $\mathbb{Z}/2[\tau]\{[2]\}$ , we only need to analyze its effect on each copy of  $C'''(0)$ , but this was already done in Section 5.4 since  $C'''(0)$  may be identified with the summand in  $\pi_{**}^{\mathbb{Q}_2}(H\mathbb{Z})$  generated by classes of the form  $\pi\tau^m$ ,  $m \geq 0$ , or equivalently, by the classes of the form  $y_m\tau^m$  for  $m$  even and  $z_m\tau^m$  for  $m$  odd. Note that any nontrivial  $d_1$ -differential over  $\mathbb{Q}_2$  involving  $\pi\tau^m$  must include it in both the source and target, so all such  $d_1$ -differentials lift to  $\mathbb{Q}$ .

The preceding discussion implies that the map

$$E_1^{\mathbb{Q}}(L) \rightarrow \prod_{\nu} E_1^{\mathbb{Q}_{\nu}}(L)$$

is injective. The  $d_1$ -differentials on  $E_1^+(L)$  are precisely the lifts of the  $d_1$ -differentials from Section 5.2 (which occur on the  $\pi$ -divisible part of the ESSS over  $\mathbb{Q}_q$ ,  $q$  odd). The  $d_1$ -differentials on  $E_1^-(L)$  are the lifts of the  $d_1$ -differentials over  $\mathbb{R}$  ([BIK22, Table 10]) and the lifts of the  $d_1$ -differentials over  $\mathbb{Q}_2$  for which the source (equivalently, the target) lift to  $\mathbb{Q}$ .

Since all of the  $d_1$ -differentials over  $\mathbb{Q}$  are lifted from  $d_1$ -differentials over the local places, the map

$$E_2^{\mathbb{Q}}(L) \rightarrow \prod_{\nu} E_2^{\mathbb{Q}_{\nu}}(L)$$

is also injective. There cannot be any higher differentials involving  $E_2^+(L)$ , since these would imply higher differentials in  $E_2^{\mathbb{Q}^q}(L)$  for  $q$  odd. On  $E_2^-(L)$ , or more generally on  $E_r^-(L)$  for  $r \geq 2$ , the nontrivial differentials are precisely the lifts of the nontrivial  $d_r$ -differentials in  $E_r^{\mathbb{R}}(L)$  described in [BIK22, Prop. 5.11].

The  $E_\infty$ -term can be described as follows. We have

$$E_\infty^{\mathbb{Q}}(L) \cong E_\infty^+(L) \oplus E_\infty^-(L).$$

The piece  $E_\infty^+(L)$  is the sum over all odd primes  $q$  of  $E_\infty^{\mathbb{F}_q}(L)$  (see Figure 14), shifted by  $(-1, 1)$ . The piece  $E_\infty^-(L)$  is the sum of  $E_\infty^{\mathbb{R}}(L)$  ([BIK22, Figs. 13-19]) and the portion of  $E_\infty^{\mathbb{Q}_2}(L)$  (Figure 16) generated by  $\pi\tau^m$  and  $\iota\pi\tau^m$ ,  $m \geq 0$ . All hidden extensions follow from comparison with the local places.

**Remark 5.4.** Since the Hasse map for  $L$  is injective on the  $E_1$ -term of the ESSS and every differential over  $\mathbb{Q}$  is lifted from a differential over some  $\mathbb{Q}_\nu$ , the Hasse map

$$\pi_{**}^{\mathbb{Q}}(L) \rightarrow \prod_{\nu} \pi_{**}^{\mathbb{Q}_\nu}(L)$$

is injective, i.e.,  $L$  satisfies the motivic Hasse principle of [OØ13, Sec. 4].

APPENDIX A. FIGURES

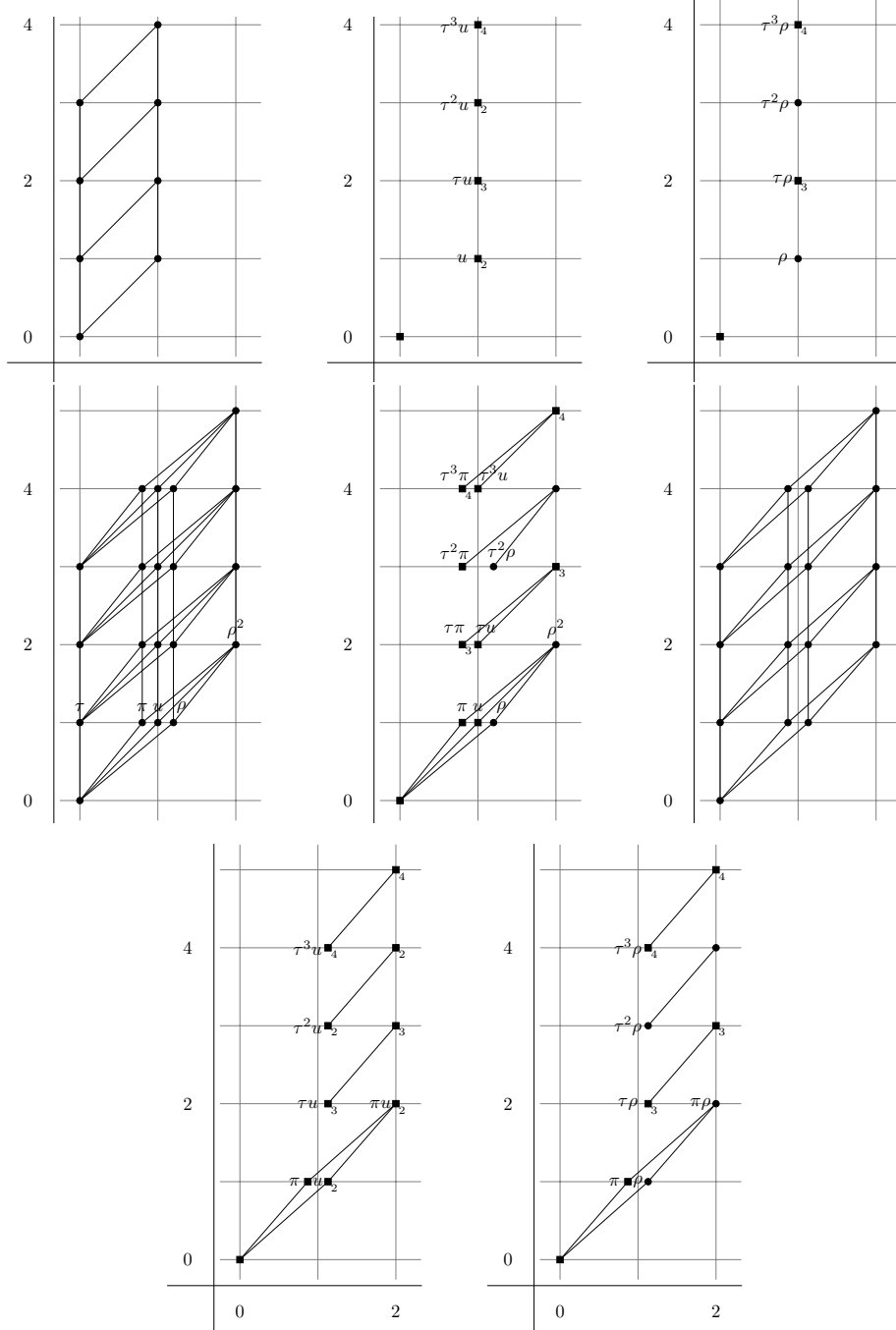


FIGURE 1. A graphical depiction of  $\pi_{***}^{\mathbb{F}_q}(H\mathbb{Z}/2)$ ,  $\pi_{***}^{\mathbb{F}_5}(H\mathbb{Z})$ ,  $\pi_{***}^{\mathbb{F}_3}(H\mathbb{Z})$ ,  $\pi_{***}^{\mathbb{Q}_2}(H\mathbb{Z}/2)$ ,  $\pi_{***}^{\mathbb{Q}_2}(H\mathbb{Z})$ ,  $\pi_{***}^{\mathbb{Q}_4}(H\mathbb{Z}/2)$ ,  $\pi_{***}^{\mathbb{Q}_5}(H\mathbb{Z})$ , and  $\pi_{***}^{\mathbb{Q}_3}(H\mathbb{Z})$ . A bullet  $\bullet$  represents  $\mathbb{Z}/2$ , a black square  $\blacksquare$  represents  $\mathbb{Z}$ , a black square with a number  $\blacksquare_n$  represents  $\mathbb{Z}/2^n$ . The  $x$  axis is  $-s$  and the  $y$  axis is  $-w$ .

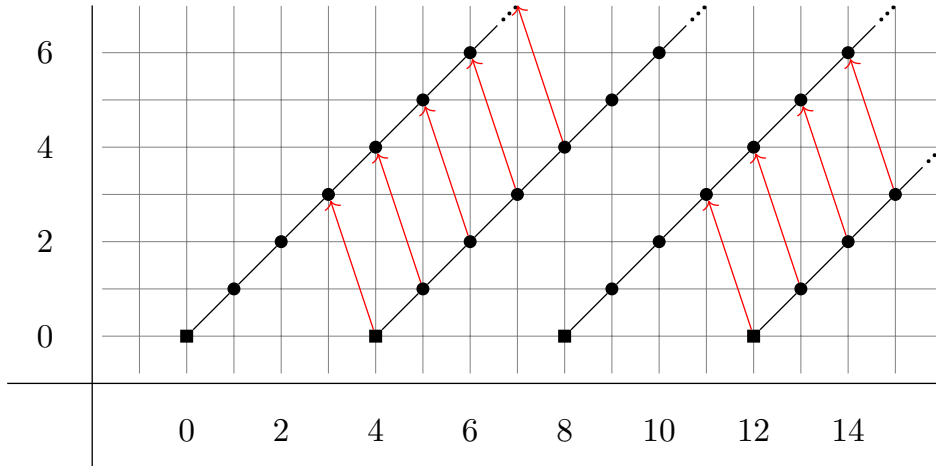


FIGURE 2. The  $E_1$ -page of the ESSS for  $kq$  over an algebraically closed field. A bullet  $\bullet$  represents  $\mathbb{Z}/2[\tau]$  and a square  $\blacksquare$  represents  $\mathbb{Z}[\tau]$ . This figure appears with generators labeled as [BIK22, Fig. 1].

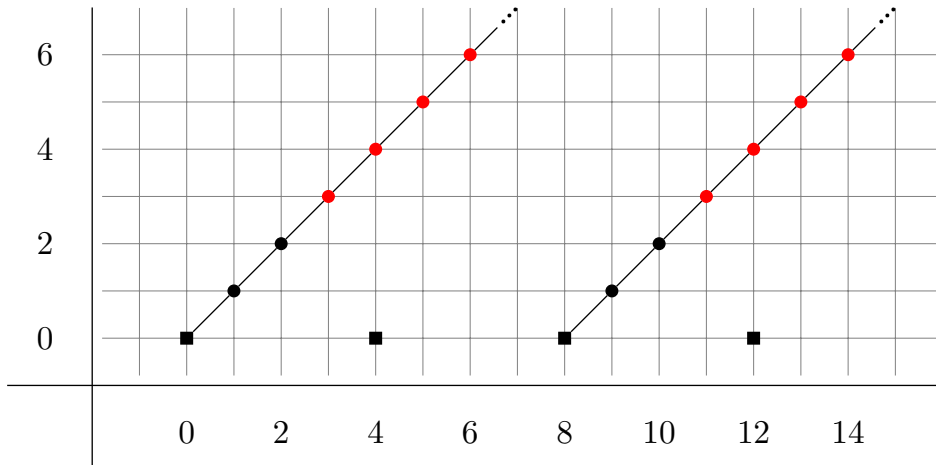


FIGURE 3. The  $E_\infty$ -page of the ESSS for  $kq$  over an algebraically closed field. A black bullet  $\bullet$  represents  $\mathbb{Z}/2[\tau]$ , a red bullet  $\bullet$  represents  $\mathbb{Z}/2$ , and a square  $\blacksquare$  represents  $\mathbb{Z}[\tau]$ . This figure appears with generators labeled as [BIK22, Fig. 2].

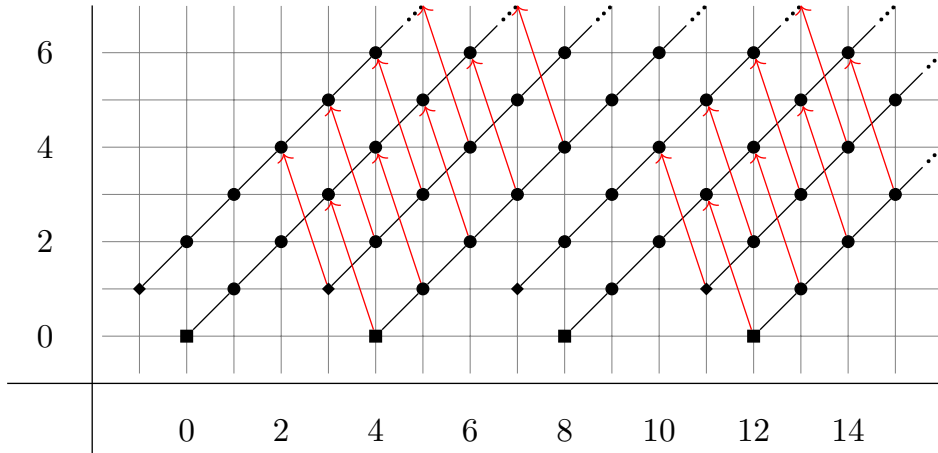


FIGURE 4. The  $E_1$ -page of the ESSS for  $kq$  over  $\mathbb{F}_q$ . A bullet  $\bullet$  represents  $\mathbb{Z}/2[\tau]$ , a square  $\blacksquare$  represents  $\mathbb{Z}$ , and a diamond  $\blacklozenge$  represents the  $u$ -divisible (if  $q \equiv 1 \pmod{4}$ ) or  $\rho$ -divisible (if  $q \equiv 3 \pmod{4}$ ) part of  $\pi_{**}^{\mathbb{F}_q}(H\mathbb{Z})$ .

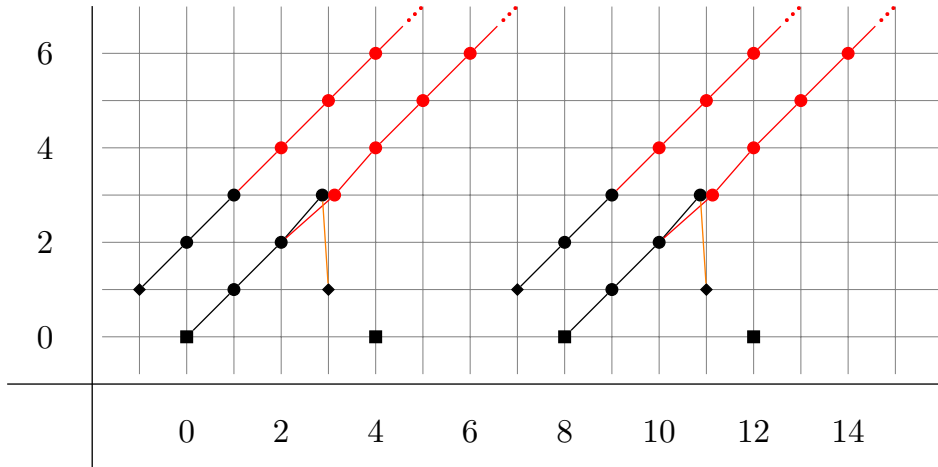


FIGURE 5. The  $E_\infty$ -page of the ESSS for  $kq$  over  $\mathbb{F}_q$ . A black bullet  $\bullet$  represents  $\mathbb{Z}/2[\tau]$ , a red bullet  $\bullet$  represents  $\mathbb{Z}/2$ , a square  $\blacksquare$  represents  $\mathbb{Z}$ , and a diamond  $\blacklozenge$  represents  $\bigoplus_{i \geq 0} \mathbb{Z}/2^{\nu(q-1)+\nu(i+1)-1}\{2\tau^i\}$ . The orange lines indicate hidden  $h$ -extensions.

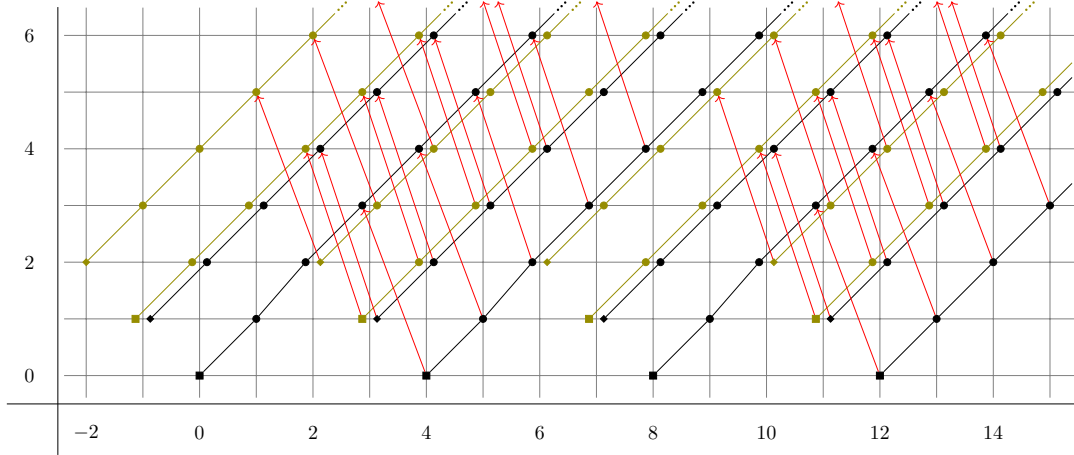


FIGURE 6. The  $E_1$ -page of the ESSS for  $kq$  over  $\mathbb{Q}_q$ . A bullet  $\bullet$  represents  $\mathbb{Z}/2[\tau]$ , a square  $\blacksquare$  represents  $\mathbb{Z}$ , and a diamond  $\blacklozenge$  represents the  $u$ -divisible (if  $q \equiv 1 \pmod{4}$ ) or  $\rho$ -divisible (if  $q \equiv 3 \pmod{4}$ ) part of  $\pi_{**}^{\mathbb{Q}_q}(H\mathbb{Z})$ . Classes in olive are  $\pi$ -divisible.

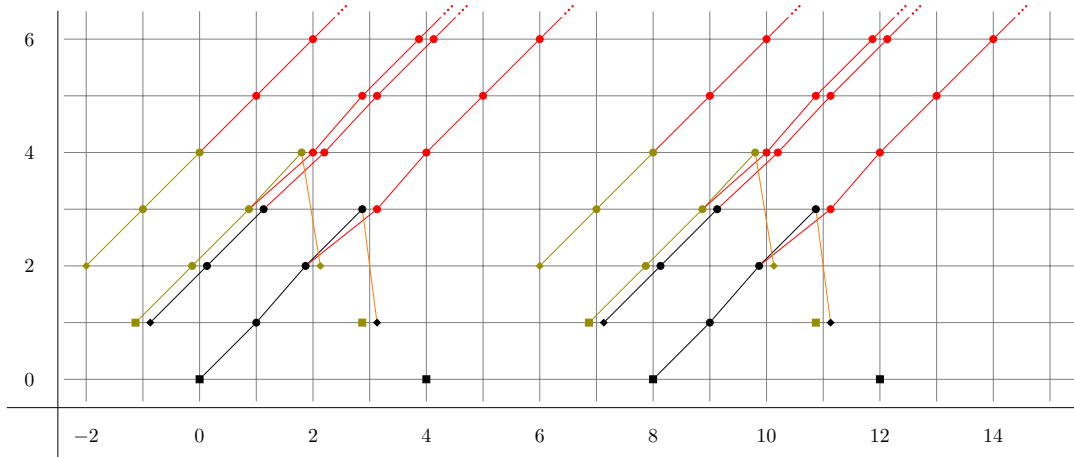


FIGURE 7. The  $E_\infty$ -page of the ESSS for  $kq$  over  $\mathbb{Q}_q$ . A black bullet  $\bullet$  represents  $\mathbb{Z}/2[\tau]$ , a red bullet  $\bullet$  represents  $\mathbb{Z}/2$ , a square  $\blacksquare$  represents  $\mathbb{Z}$ , and a diamond  $\blacklozenge$  represents the group obtained from the  $u$ -divisible (if  $q \equiv 1 \pmod{4}$ ) or  $\rho$ -divisible (if  $q \equiv 3 \pmod{4}$ ) part of  $\pi_{**}^{\mathbb{F}_q}(H\mathbb{Z})$  by dividing the order by two. Classes in olive are  $\pi$ -divisible, and orange lines indicate hidden h-extensions.

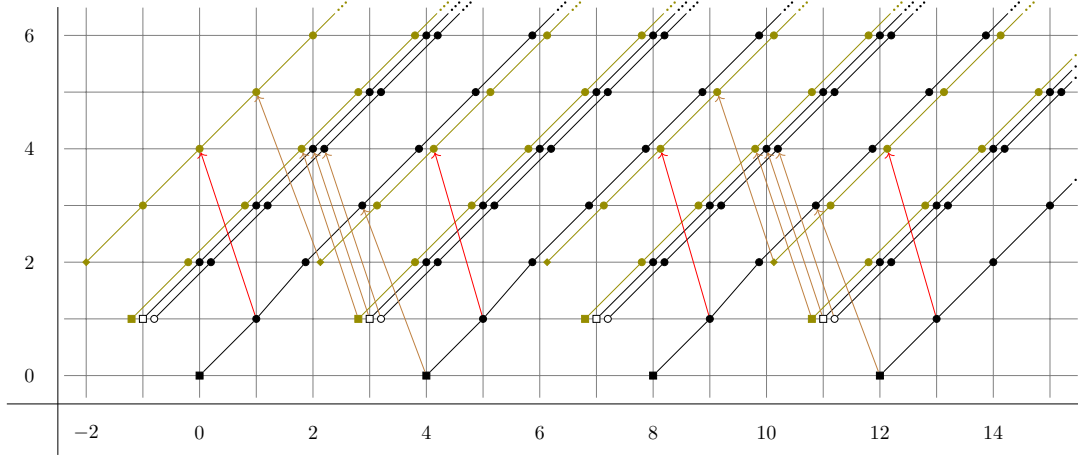


FIGURE 8. The  $E_1$ -page of the ESSS for  $kq$  over  $\mathbb{Q}_2$ . A bullet  $\bullet$  represents  $\mathbb{Z}/2[\tau]$ , a circle  $\circ$  represents  $\mathbb{Z}/2[\tau^2]\{\rho\}$ , a black square  $\blacksquare$  represents  $\mathbb{Z}$ , a rectangle  $\square$  represents  $\mathbb{Z}[\tau^2]\{\tau u\} \oplus \mathbb{Z}\{u\}$ , a diamond  $\blacklozenge$  represents  $\pi_{-2,*}^{\mathbb{Q}_2}(H\mathbb{Z})$ , and an olive square  $\blacksquare$  represents the  $\pi$ -divisible part of  $\pi_{-1,*}^{\mathbb{Q}_2}(H\mathbb{Z})$ . Classes in olive are  $\pi$ -divisible. The differentials are  $h_1$ -periodic; we only draw the first occurrences.

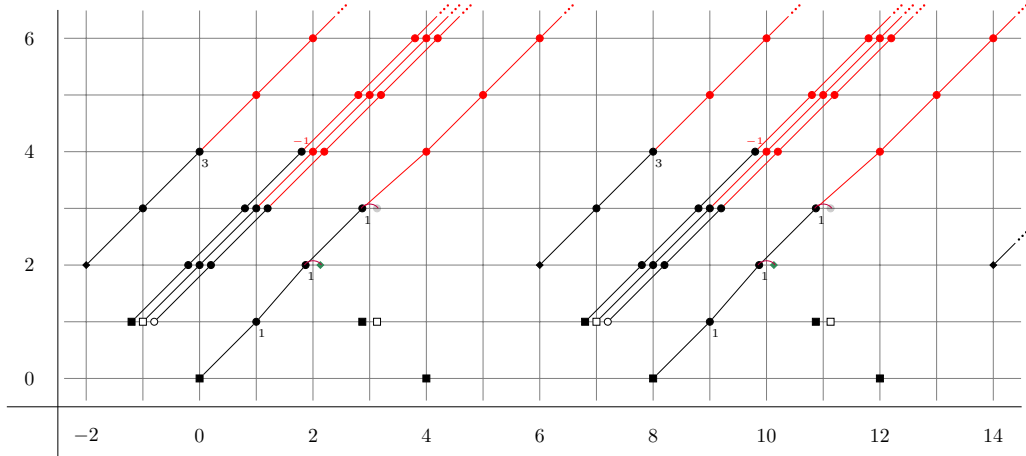


FIGURE 9. The  $E_\infty$ -page of the ESSS for  $kq$  over  $\mathbb{Q}_2$ . A bullet  $\bullet$  represents  $\mathbb{Z}/2[\tau]$ , a red bullet  $\bullet$  represents  $\mathbb{Z}/2$ , a bullet with subscript  $\bullet_n$  represents  $\mathbb{Z}/2[\tau^4]\{1, \tau^n\}$ , a bullet with label  $-1$  represents  $\mathbb{Z}/2[\tau]\{\tau^2\} \oplus \mathbb{Z}/2$ , a circle  $\circ$  represents  $\mathbb{Z}/2[\tau^2]\{\rho\}$ , a square  $\blacksquare$  represents  $\mathbb{Z}$ , a rectangle  $\square$  represents  $\mathbb{Z}[\tau^2]\{\tau u\} \oplus \mathbb{Z}\{u\}$ , a diamond  $\blacklozenge$  represents  $\pi_{-2,*}^{\mathbb{Q}_2}(H\mathbb{Z})$ , and a dark green diamond  $\blacklozenge$  represents  $2\pi_{-2,*}^{\mathbb{Q}_2}(H\mathbb{Z})$ . A curve represents  $(\mathbb{Z}/2[\tau^4])^2$  which is some linear combination of the classes it connects (a faded bullet represents an  $E_1$ -page class that does not exist on the  $E_2$ -page).

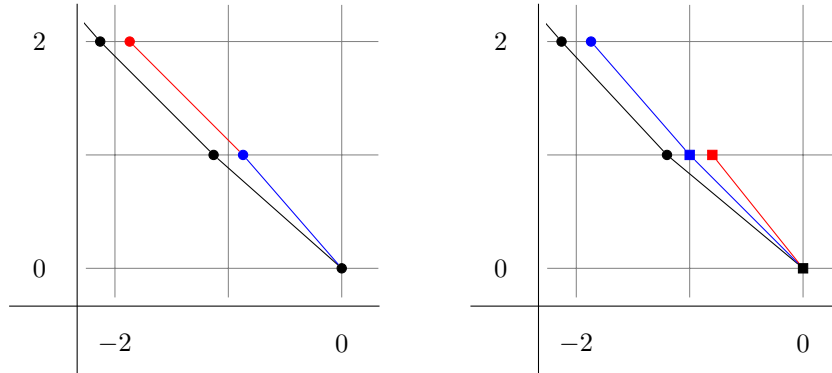


FIGURE 10. A graphical depiction of  $\pi_{**}^{\mathbb{Q}}(H\mathbb{Z}/2)$  (left) and  $\pi_{**}^{\mathbb{Q}}(H\mathbb{Z})$  (right). In the left-hand picture, a black bullet  $\bullet$  represents  $\mathbb{Z}/2[\tau]$ , a blue bullet  $\bullet$  represents  $\bigoplus_{q \text{ prime}} \mathbb{Z}/2[\tau]\{[q]\}$ , and a red bullet  $\bullet$  represents  $\bigoplus_{q \text{ odd}} \mathbb{Z}/2[\tau]\{a_q\}$ . In the right-hand picture, a black square  $\blacksquare$  represents  $\mathbb{Z}$ , a black bullet  $\bullet$  represents  $\mathbb{Z}/2[\tau^2]$ , a blue square  $\blacksquare$  represents  $\bigoplus_{q \text{ odd}} \mathbb{Z}\{[q]\}$ , a red square  $\blacksquare$  represents  $C'''(0)$ , and a blue bullet  $\bullet$  represents  $\bigoplus_{q \text{ odd}} \bigoplus_{i \geq 0} \mathbb{Z}/2^{s_q(i)}\{[q]x_q\tau^i\}$ .

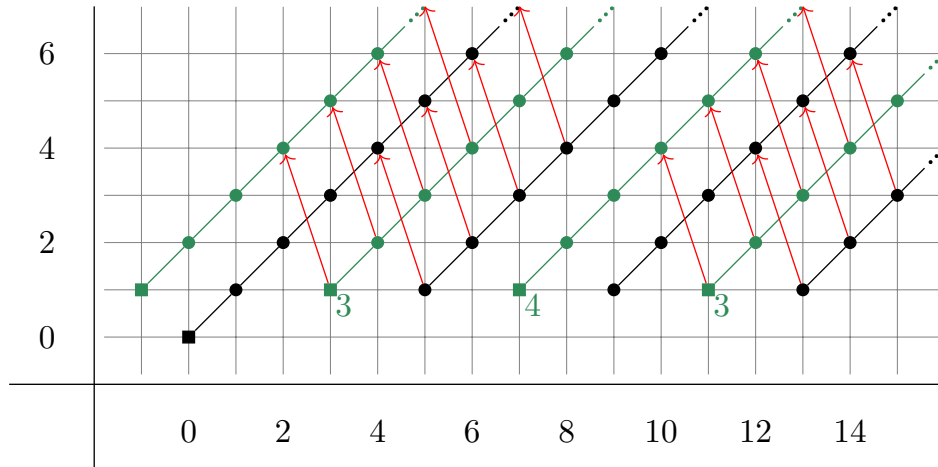


FIGURE 11. The  $E_1$ -page of the ESSS for  $L$  over algebraically closed fields. A bullet  $\bullet$  represents  $\mathbb{Z}/2[\tau]$ , a square  $\blacksquare$  represents  $\mathbb{Z}[\tau]$ , and a square with the positive integer  $n$  as its right subscript  $\blacksquare_n$  represents  $\mathbb{Z}/2^n[\tau]$ . Elements of the form  $\iota x$  appear in dark green. This figure appears with generators labeled as [BIK22, Fig. 3].

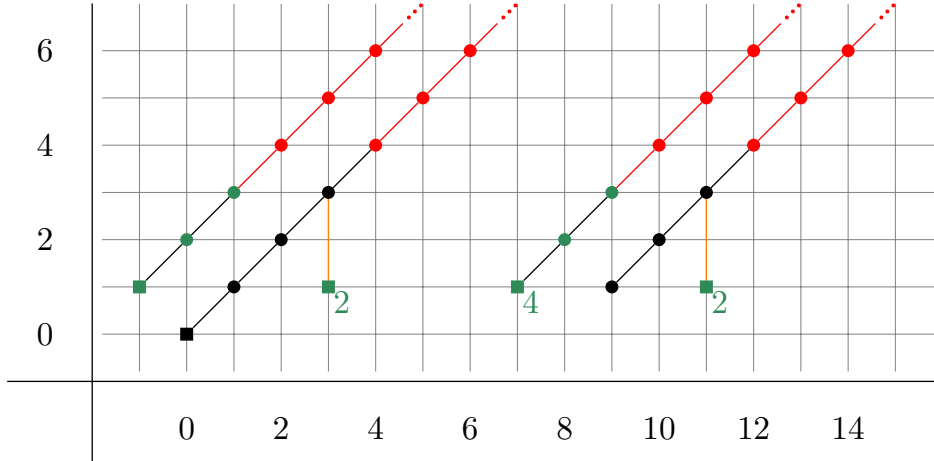


FIGURE 12. The  $E_\infty$ -page of the ESSS for  $L$  over algebraically closed fields. A bullet  $\bullet$  represents  $\mathbb{Z}/2[\tau]$ , a red bullet  $\bullet$  represents  $\mathbb{Z}/2$ , a square  $\blacksquare$  represents  $\mathbb{Z}[\tau]$ , and a square with the positive integer  $n$  as its right subscript  $\blacksquare_n$  represents  $\mathbb{Z}/2^n[\tau]$ . Hidden extensions are depicted with orange lines. This figure appears with generators labeled as [BIK22, Fig. 3].

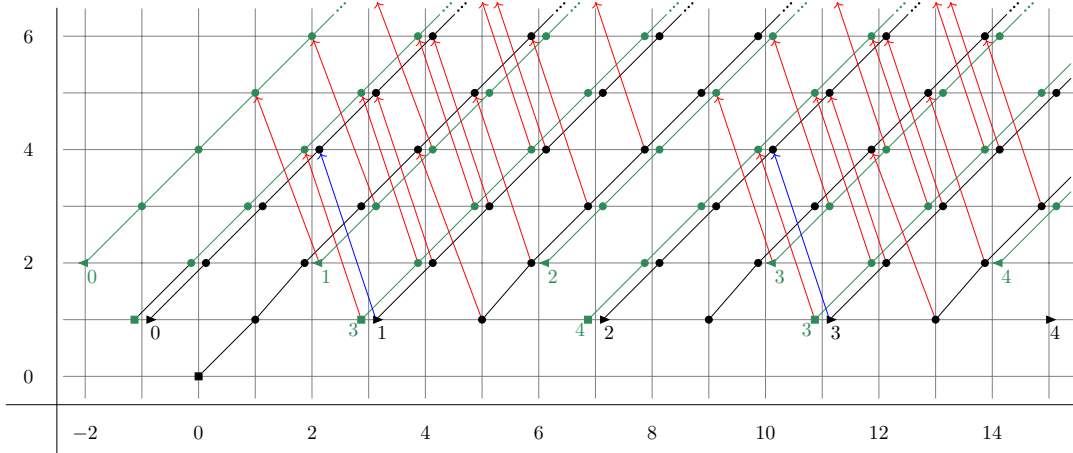


FIGURE 13. The  $E_1$ -page of the ESSS for  $L$  over  $\mathbb{F}_q$ . A bullet  $\bullet$  represents  $\mathbb{Z}/2[\tau]$ , a square  $\blacksquare$  represents  $\mathbb{Z}$ , a square with the positive integer  $n$  as its left subscript  ${}^n\blacksquare$  represents  $\mathbb{Z}/2^n$ , an isosceles triangle with apex pointing right and nonnegative integer  $n$  as its right subscript  $\blacktriangleright_n$  represents  $K_q(n)$ , and an isosceles triangle with apex pointing left and nonnegative integer  $n$  as its right subscript  $\blacktriangleleft_n$  represents  $C_q(n)$ . Elements of the form  $\iota x$  appear in dark green.

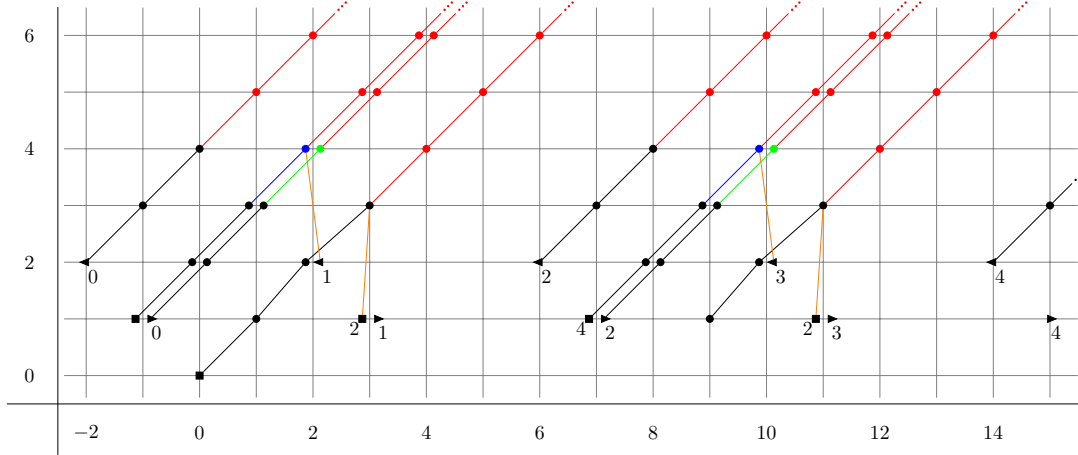


FIGURE 14. The  $E_\infty$ -page of the ESSS for  $L$  over  $\mathbb{F}_q$ . A bullet  $\bullet$  represents  $\mathbb{Z}/2[\tau]$ , a red bullet  $\bullet$  represents  $\mathbb{Z}/2$ , a blue bullet  $\bullet$  represents  $\mathbb{Z}/2\{1\} \oplus \mathbb{Z}/2[\tau]\{\tau^2\}$ , a green bullet  $\bullet$  represents the cokernel of the corresponding green  $d_1$ -differential, a square  $\square$  represents  $\mathbb{Z}$ , a square with the positive integer  $n$  as its left subscript represents  $\mathbb{Z}/2^n$ , an isosceles triangle with apex pointing right and nonnegative integer  $n$  as its right subscript  $\blacktriangleright_n$  represents  $\tilde{K}_q(n)$ , and an isosceles triangle with apex pointing left and nonnegative integer  $n$  as its right subscript  $\blacktriangleleft_n$  represents  $\tilde{C}_q(n)$ . Hidden extensions are depicted with orange lines.

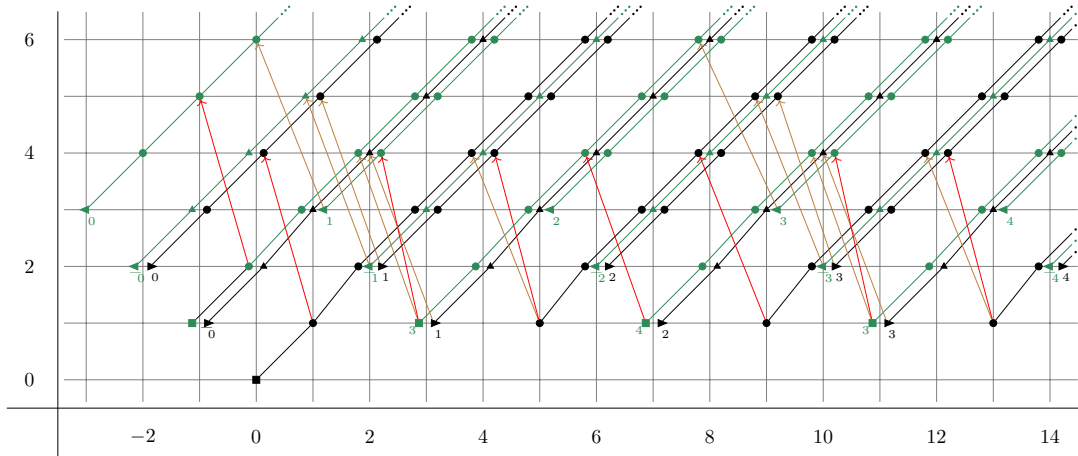


FIGURE 15. The  $E_1$ -page of the ESSS for  $L$  over  $\mathbb{Q}_2$ . A bullet  $\bullet$  represents  $\mathbb{Z}/2[\tau]$ , a triangle  $\blacktriangle$  represents  $(\mathbb{Z}/2[\tau])^3$ , a square  $\blacksquare$  represents  $\mathbb{Z}$ , a square with the positive integer  $n$  as its left subscript  $n\blacksquare$  represents  $\mathbb{Z}/2^n$ , an isosceles triangle with apex pointing left and nonnegative integer  $n$  as its right subscript  $\blacktriangleleft_n$  ( $\blacktriangleleft_n$ ) represents  $C_2(n)$  ( $\underline{C}_2(n)$ ), and an isosceles triangle with apex pointing right and nonnegative integer  $n$  as its right subscript  $\blacktriangleright_n$  ( $\blacktriangleright_n$ ) represents  $K_2(n)$  ( $\underline{K}_2(n)$ ). Elements of the form  $\iota x$  appear in dark green. The differentials are  $h_1$ -periodic; we only draw the first occurrences.

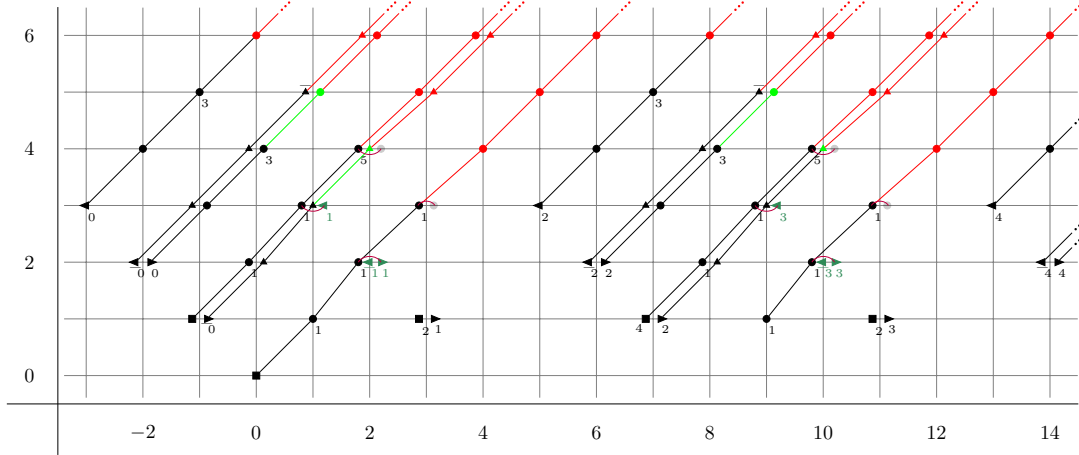


FIGURE 16. The  $E_\infty$ -page of the ESSS for  $L$  over  $\mathbb{Q}_2$ . A bullet  $\bullet$  represents  $\mathbb{Z}/2[\tau]$ , a red bullet  $\bullet$  represents  $\mathbb{Z}/2$ , a green bullet  $\bullet$  represents  $\mathbb{Z}/2[\tau^4]$ , a bullet with subscript  $\bullet_n$  represents  $\mathbb{Z}/2[\tau^4]\{1, \tau^n\}$ , a triangle  $\blacktriangle$  represents  $(\mathbb{Z}/2[\tau])^3$ , a red triangle  $\blacktriangle$  represents  $(\mathbb{Z}/2)^3$ , a overlined triangle  $\overline{\blacktriangle}$  represents  $\mathbb{Z}/2[\tau^2] \oplus \mathbb{Z}/2[\tau^2]\{\tau^3\}$ , a green triangle  $\blacktriangle$  represents  $\mathbb{Z}/2[\tau^2] \oplus \mathbb{Z}/2[\tau^2]\{\tau^3\} \oplus \mathbb{Z}/2[\tau^4]\{1, \tau, \tau^3\}$ , a square  $\blacksquare$  represents  $\mathbb{Z}$ , a square with the positive integer  $n$  as its left subscript  $n\blacksquare$  represents  $\mathbb{Z}/2^n$ , an isosceles triangle with apex pointing left and nonnegative integer  $n$  as its right subscript  $\blacktriangleleft_n$  ( $\blacktriangleleft_n, \blacktriangleleft_n, \blacktriangleleft_n$ ) represents  $C_2(n)$  ( $\tilde{C}_2(n), \underline{C}_2(n), \tilde{\underline{C}}_2(n)$ ), and an isosceles triangle with apex pointing right and nonnegative integer  $n$  as its right subscript  $\blacktriangleright_n$  ( $\blacktriangleright_n, \blacktriangleright_n$ ) represents  $K_2(n)$  ( $\underline{K}_2(n), \tilde{K}_2(n)$ ). A curve represents  $(\mathbb{Z}/2[\tau^4])^2$  which is some linear combination of the classes it connects (a faded bullet represents a  $E_1$ -page class that does not exist on the  $E_2$ -page).

REFERENCES

- [AM17] Michael Andrews and Haynes Miller. Inverting the Hopf map. *J. Topol.*, 10(4):1145–1168, 2017. 1
- [ARØ20] Alexey Ananyevskiy, Oliver Röndigs, and Paul Arne Østvær. On very effective hermitian  $K$ -theory. *Math. Z.*, 294(3-4):1021–1034, 2020. 2, 6
- [Bac22] Tom Bachmann.  $\eta$ -periodic motivic stable homotopy theory over Dedekind domains. *J. Topol.*, 15(2):950–971, 2022. 2
- [BCQ21] William Balderrama, Dominic Leon Culver, and J.D. Quigley. The motivic lambda algebra and motivic Hopf invariant one problem. *arXiv preprint arXiv:2112.07479*, 2021. 1, 4
- [BH20] Tom Bachmann and Michael J Hopkins.  $\eta$ -periodic motivic stable homotopy theory over fields. *arXiv preprint arXiv:2005.06778*, 2020. 2, 6
- [BI22] Eva Belmont and Daniel C. Isaksen.  $\mathbb{R}$ -motivic stable stems. *J. Topol.*, 15(4):1755–1793, 2022. 1, 3
- [BIK22] Eva Belmont, Daniel C Isaksen, and Hana Jia Kong.  $\mathbb{R}$ -motivic  $v_1$ -periodic homotopy. *arXiv preprint arXiv:2204.05937*, 2022. 2, 3, 4, 5, 6, 7, 12, 14, 15, 17, 18, 19, 21, 25, 26
- [BK05] A. J. Berrick and M. Karoubi. Hermitian  $K$ -theory of the integers. *Amer. J. Math.*, 127(4):785–823, 2005. 4
- [Boa99] J. Michael Boardman. Conditionally convergent spectral sequences. In *Homotopy invariant algebraic structures (Baltimore, MD, 1998)*, volume 239 of *Contemp. Math.*, pages 49–84. Amer. Math. Soc., Providence, RI, 1999. 7
- [CQ21] Dominic Leon Culver and J.D. Quigley.  $kq$ -resolutions I. *Trans. Amer. Math. Soc.*, 374(7):4655–4710, 2021. 1, 2
- [DI10] Daniel Dugger and Daniel C. Isaksen. The motivic Adams spectral sequence. *Geom. Topol.*, 14(2):967–1014, 2010. 1, 7, 10
- [DI17a] Daniel Dugger and Daniel Isaksen. Low-dimensional Milnor-Witt stems over  $\mathbb{R}$ . *Ann. K-Theory*, 2(2):175–210, 2017. 3
- [DI17b] Daniel Dugger and Daniel C. Isaksen.  $\mathbb{Z}/2$ -equivariant and  $\mathbb{R}$ -motivic stable stems. *Proc. Am. Math. Soc.*, 145(8):3617–3627, 2017. 1
- [Fri76] Eric M. Friedlander. Computations of  $K$ -theories of finite fields. *Topology*, 15:87–109, 1976. 4
- [GI15] Bertrand J. Guillou and Daniel C. Isaksen. The  $\eta$ -local motivic sphere. *J. Pure Appl. Algebra*, 219(10):4728–4756, 2015. 1
- [GI16] Bertrand J. Guillou and Daniel C. Isaksen. The  $\eta$ -inverted  $\mathbb{R}$ -motivic sphere. *Algebr. Geom. Topol.*, 16(5):3005–3027, 2016. 1
- [Hil11] Michael A. Hill. Ext and the motivic Steenrod algebra over  $\mathbb{R}$ . *J. Pure Appl. Algebra*, 215(5):715–727, 2011. 3, 7, 8
- [HKO11] P. Hu, I. Kriz, and K. Ormsby. Convergence of the motivic Adams spectral sequence. *J. K-Theory*, 7(3):573–596, 2011. 7
- [IØ20] Daniel C. Isaksen and Paul Arne Østvær. Motivic stable homotopy groups. In *Handbook of homotopy theory*, CRC Press/Chapman Hall Handb. Math. Ser., pages 757–791. CRC Press, Boca Raton, FL, [2020] ©2020. 7
- [Isa19] Daniel C. Isaksen. Stable stems. *Mem. Amer. Math. Soc.*, 262(1269):viii+159, 2019. 1
- [IWX20] Daniel C Isaksen, Guozhen Wang, and Zhouli Xu. More stable stems. *arXiv preprint arXiv:2001.04511*, 2020. 1
- [KQ22] Hana Jia Kong and J.D. Quigley.  $v_1$ -periodic motivic homotopy over rings of integers of number fields. *In preparation*, 2022. 5
- [KRØ20] Jonas Irgens Kylling, Oliver Röndigs, and Paul Arne Østvær. Hermitian  $K$ -theory, Dedekind  $\zeta$ -functions, and quadratic forms over rings of integers in number fields. *Camb. J. Math.*, 8(3):505–607, 2020. 3, 5
- [Kyl15] Jonas Irgens Kylling. Hermitian  $K$ -theory of finite fields via the motivic Adams spectral sequence. Master’s thesis, University of Oslo, Norway, 2015. 3, 4, 7, 10, 11, 13
- [Lev08] Marc Levine. The homotopy coniveau tower. *J. Topol.*, 1(1):217–267, 2008. 6
- [Mil70] John Milnor. Algebraic  $K$ -theory and quadratic forms. *Invent. Math.*, 9:318–344, 1969/70. 7
- [Mor12] Fabien Morel.  $\mathbb{A}^1$ -algebraic topology over a field, volume 2052 of *Lecture Notes in Mathematics*. Springer, Heidelberg, 2012. 1
- [MV99] Fabien Morel and Vladimir Voevodsky.  $\mathbb{A}^1$ -homotopy theory of schemes. *Publ. Math., Inst. Hautes Étud. Sci.*, 90:45–143, 1999. 1

- [OØ13] Kyle M. Ormsby and Paul Østvær. Motivic Brown-Peterson invariants of the rationals. *Geom. Topol.*, 17(3):1671–1706, 2013. 3, 4, 7, 8, 9, 10, 11, 14, 19
- [OØ14] Kyle M. Ormsby and Paul Arne Østvær. Stable motivic  $\pi_1$  of low-dimensional fields. *Adv. Math.*, 265:97–131, 2014. 1
- [OR20] Kyle Ormsby and Oliver Röndigs. The homotopy groups of the  $\eta$ -periodic motivic sphere spectrum. *Pacific J. Math.*, 306(2):679–697, 2020. 1
- [Orm11] Kyle M. Ormsby. Motivic invariants of  $p$ -adic fields. *J. K-Theory*, 7(3):597–618, 2011. 3, 8
- [Qui21a] J.D. Quigley. Motivic Mahowald invariants over general base fields. *Doc. Math.*, 26:561–582, 2021. 2, 3
- [Qui21b] J.D. Quigley. Real motivic and  $C_2$ -equivariant Mahowald invariants. *J. Topol.*, 14(2):369–418, 2021. 2, 3
- [RØ16] Oliver Röndigs and Paul Østvær. Slices of Hermitian  $K$ -theory and Milnor’s conjecture on quadratic forms. *Geom. Topol.*, 20(2):1157–1212, 2016. 3, 4, 13
- [RSØ19] Oliver Röndigs, Markus Spitzweck, and Paul Østvær. The first stable homotopy groups of motivic spheres. *Ann. Math. (2)*, 189(1):1–74, 2019. 1, 3, 5, 6
- [RSØ21] Oliver Röndigs, Markus Spitzweck, and Paul Arne Østvær. The second stable homotopy groups of motivic spheres. *arXiv preprint arXiv:2103.17116*, 2021. 1, 3, 5
- [RW00] J. Rognes and C. Weibel. Two-primary algebraic  $K$ -theory of rings of integers in number fields. *J. Amer. Math. Soc.*, 13(1):1–54, 2000. Appendix A by Manfred Kolster. 4
- [Voe03] Vladimir Voevodsky. Reduced power operations in motivic cohomology. *Publ. Math., Inst. Hautes Étud. Sci.*, 98:1–57, 2003. 7
- [Voe11] Vladimir Voevodsky. On motivic cohomology with  $\mathbb{Z}/l$ -coefficients. *Ann. Math. (2)*, 174(1):401–438, 2011. 7
- [Wil16] Glen M. Wilson. *Motivic stable stems over finite fields*. ProQuest LLC, Ann Arbor, MI, 2016. Thesis (Ph.D.)—Rutgers The State University of New Jersey - New Brunswick. 1
- [Wil18] Glen Matthew Wilson. The eta-inverted sphere over the rationals. *Algebr. Geom. Topol.*, 18(3):1857–1881, 2018. 1, 17
- [WØ17] Glen Matthew Wilson and Paul Østvær. Two-complete stable motivic stems over finite fields. *Algebr. Geom. Topol.*, 17(2):1059–1104, 2017. 1, 3, 7

INSTITUTE FOR ADVANCED STUDY

*Email address:* hana.jia.kong@gmail.com

MAX PLANCK INSTITUTE FOR MATHEMATICS

*Email address:* jqigley1993@gmail.com